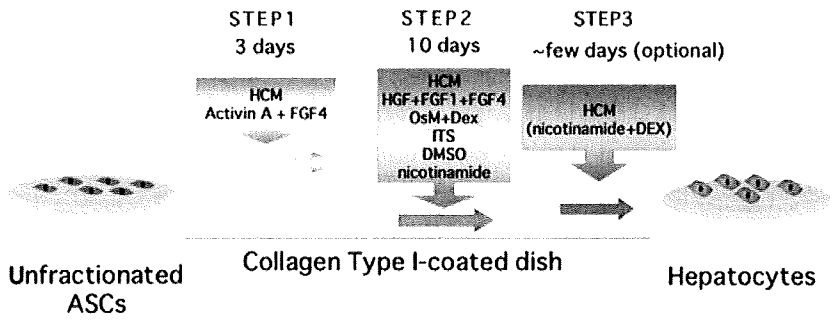

Figure 1 Improved and modified hepatogenic induction strategy. At present, approximately 2 weeks are required to induce hepatogenic characteristics in adipose-derived stem cells (ASC). Unfractionated ASC were plated on collagen type I-coated dishes and were treated with Activin A and FGF4 at step 1, followed by step 2, treatment with hepatocyte growth factor (HGF), fibroblast growth factor (FGF)1, FGF4, oncostatin M (OsM), dexamethasone, insulin-transferrin-selenium (ITS), dimethyl sulfoxide (DMSO), and nicotinamide. At this point, cells may be maintained a few days in hepatocyte culture medium (HCM) alone (or optionally supplemented with 10^{-6} mol/L dexamethasone and 0.05 mmol/L nicotinamide). MSC, mesenchymal stem cells.

lymphocyte antigen [HLA I]) and no MHC II (HLA II) expression, therefore reducing the risk of allogenic transplant rejection.[20–27]

Currently, attention is being given to adipose tissue (AT) as a source of MSC for regenerative medicine. From adipose tissue, a sufficient number of stem cells for a stem cell-based therapy may be obtained without invasiveness or damage to a patient's health. We have already demonstrated that human ASC have the ability to give rise to hepatocyte-like cells and that CD105 is a candidate mesenchymal stem cell marker.[19] However, this *in vitro* differentiation method is not applicable to a practical, clinical use, as more than 1 month is required to induce ASC into cells with hepatic functions.

In the present study, we evaluate the therapeutic potential of ASC-derived hepatocyte-like cells after transplantation into mice with liver injury. Clinical applications in the future would require a special approach, such as shortening as much as possible *ex vivo* manipulations, including cultivation and direct hepatic fate. Therefore, we improved and modified our hepatocyte differentiation strategy, based on the current knowledge on *in vivo* mouse fetal liver development. At present, a period as short as 13 days is required and that strategy is enriched by pretreatment with Activin A (PeproTech, EC, London, UK) and fibroblast growth factor (FGF)4 (PeproTech) (one of the factors secreted by septum transversum mesenchyme (STM) and cardiogenic mesoderm at the early stage of endoderm development *in vivo*). Additionally, we reorganized the content of the growth factor cocktail and enriched it with the addition of dimethyl sulfoxide (DMSO), nicotinamide and insulin-transferrin-selenium. Using the present protocol, we obtained functional hepatocyte-like cells in a much shorter period of time. Finally, we transplanted ASC-derived hepatocyte-like cells into immunodeficient mice with liver injury/non-severe acute liver injury. Our results showed a significant decrease of ammonia, aspartate aminotransferase (AST), alanine aminotransferase (ALT), and uric acid (UA) in the blood plasma of mice after ASC-derived hepatocyte-like cell transplantation. The results show a very important step towards future establishment of an alternative and successful therapy for liver disease.

Methods

Isolation and culturing of ASC

Adipose-derived stem cells were derived from abdominal subcutaneous adipose tissue, which was obtained from two female gastric cancer patients (Donor #1 [36 years old] and Donor #2 [45 years old]), undergoing gastrectomy at the International Medical Center of Japan, Tokyo. The hospital's committee of ethics approved this study, and informed consent was obtained from both patients. Adipose tissue was processed as previously described.[19] For *in vitro* differentiation, the cells (ASC062801, ASC012202, ASC0025) obtained from DS Pharma Biomedical Co., Osaka, Japan) were also analyzed.

Hepatic differentiation

At passage five to 10, the cells were plated on collagen type I-coated dishes at a concentration of $3.0–4.0 \times 10^4$ cells/cm^2 (Fig. 1). When the cells reached confluency, hepatogenic induction was carried out over a period of 2 weeks. First, the cells were treated for 3 days with DMEM (GibcoBRL, Tokyo, Japan) (serum free) supplemented with 20 ng/mL Activin A and 20 ng/mL FGF4 (PeproTech EC, London, UK). Afterwards, the cells were cultured for 10 days in a hepatocyte culture medium (HCM), containing 5 μg/mL transferrin, 10^{-6} mol/L hydrocortisone-21-hemisuccinate, 0.5 mg/mL bovine serum albumin, 2 mmol/L ascorbic acid, 20 ng/mL epidermal growth factor, 5 μg/mL insulin, 50 μg/mL gentamicin (Cambrex Corp., Walkersville, MD, USA) and supplemented with 150 ng/mL hepatocyte growth factor (HGF), 100 ng/mL FGF1, 25 ng/mL FGF4, 30 ng/mL oncostatin M (OsM; PeproTech), (2×10^{-5} mol/L) dexamethasone (Dex; Sigma, Tokyo, Japan), 1 × insulin-transferrin-selenium (ITS; Gibco), 0.05 mmol/L nicotinamide (Sigma), and 0.1% DMSO (Sigma). For the next few days, the cells were maintained with HCM alone. For *in vivo* transplantation, hepatocyte-like cells from two donors (#1 and #2) were harvested by treatment with a 0.05% collagenase/1000 U/mL dispase solution for 3–5 min, dissolved in

PBS (–) and injected intravenously into mice with liver injury caused by CCl_4 injection.

Quantitative real-time PCR

In order to confirm the regulation of the hepatocyte-specific genes in ASC-derived hepatocytes, we performed real-time polymerase chain reaction (PCR) for albumin (ALB) and tryptophan 2,3-dioxygenase (TDO2), with glyceraldehyde-3-phosphate dehydrogenase (GAPDH) as a reference gene. After retro-transcription, cDNA was subjected to real-time PCR by using Platinum Quantitative PCR Super Mix-UDG (Invitrogen, Tokyo, Japan) and specific primers for ALB (NM_000477): F:GTCACCAAATG CTGCACAGA, R:ACGAGCTCAACAAGTGCAGT for TDO2 (NM_005651): F:GTGTGCATGGTGCACAGAAT, R:GGGTT CATCTTCGGTATCCA, for FOXA2 (NM_021784): F:GGGA GCGGTGAAGATGGAAG, R:TGCCAGCGCCCACGTA and for GAPDH (NG_007073): F:GAAGGTGAAGGTCGGAGT, and R:GAAGATGGTGATGGGATTTC, based on the human genome database. The PCR conditions were as follows: denaturation at 95°C for 30 s, annealing at 56°C or 60°C for 30 s, and extension at 72°C for 30 s for up to 45 cycles. Real-time PCR was carried out by using the Applied Biosystems (Tokyo, Japan) PRISM 7700 Sequence Detection System.

Immunofluorescence

Cells were fixed in 4% formaldehyde for 10 min, followed by incubation with Protein Block (DakoCytomation, Carpinteria, CA, USA) for 30 min. ASC-derived hepatocytes were analyzed by immunohistochemistry using monoclonal anti-human specific albumin ALB (clone HAS-11, 1:250; Sigma) antibody overnight at 4°C. The Alexa Fluor 488 (green, 1:1000)-conjugated secondary antibody (Invitrogen, Tokyo, Japan) was applied for 30 min. Nuclei staining was performed using 4,6-diamidino-2-phenylindole (DAPI; Vector Laboratories, Burlingame, CA, USA).

Albumin production

Albumin production was evaluated by enzyme linked immunosorbent assay (ELISA, E80-129; Bethyl Laboratories, Montgomery, TX, USA). The antibody is human specific and does not cross-react with mouse, rat, bovine, goat, and pig albumin. Briefly, the supernatant during hepatogenic induction was collected every 3 days at days 3, 6 and 9, and ELISA assay was performed. Data are reported as the mean ± SD and were analyzed by Student's *t*-test, $n = 3$ ($^*P < 0.05$).

ASC-derived hepatocyte transplantation into mice with CCl_4-induced injury

Animal studies were carried out in compliance with the guidelines of the Institute for Laboratory Animal Research, National Cancer Center Research Institute. Six-week-old female BALB/c nude mice (CLEA Japan Inc., Tokyo, Japan) were used. An acute liver failure model was produced by giving one dose of CCl_4. At day 0, mice underwent i.p. injection of 100 μL/20 g bodyweight of olive oil containing 10 μL CCl_4. At day 1, mice underwent transplantation of ASC-derived hepatocyte-like cells (Donor #1 ($n = 4$), or Donor #2 ($n = 4$) at a concentration of 1.5×10^6 cells per mouse (0.2 mL cell suspension was injected through the tail vein). As a control, non-transplanted CCl_4-treated mice ($n = 3$) and non-transplanted CCl_4-non-treated (olive oil) ($n = 3$) mice were used. Twenty-four hours after transplantation, blood serum was collected and evaluated for biochemical parameters, such as AST, ALT, UA and ammonia concentration levels.

Assessment of liver functions

Blood samples were obtained from each mouse, centrifuged for 20 min at 400 *g* and serum was collected. Serum samples were tested for ammonia concentration level by using the Ammonia Test-Wako (Wako Pure Chemicals, Tokyo, Japan). The concentration of markers of liver injury such as ALT, AST and UA was analyzed by using a FUJIFILM DRI-CHEM 3500 machine and FUJI DRI-CHEM Slides for ALT/ALT-PIII, AST/AST-PIII, and UA-PIII, respectively (Fujifilm Co., Tokyo, Japan).

Statistical analysis

The results are given as the mean ± SD. Statistical analyses were conducted using either the variance with the Bonferroni correction for multiple comparisons or the Student's *t*-test. The statistical analysis of quantitative relative expression was evaluated by using the Pair Wise Fixed Reallocation Randomization Test©, Relative Expression Software Tool-XL = REST-XL© (http://www.gene-quantification.info/). A P value < 0.05 was considered significant.

Results

Hepatic fate specification of ASC

A direct fate hepatic specification (Fig. 1) was performed within 13 days. After that, ASC-derived hepatocyte-like cells could be maintained for a few days in HCM alone (optionally supplemented with Dex 10^{-8} mol/L and nicotinamide 0.05 mmol/L). After 3 days of pretreatment with FGF4 and Activin A, ASC expressed FOXA2 (Fig. 2a), the expression of which was decreased at day 6 of the induction system (3 days of pretreatment with FGF4 and Activin A, followed by 3 days of treatment with a cocktail containing HGF, FGF1, FGF4, OsM, Dex, ITS, DMSO and nicotinamide) (Fig. 2a). FOXA2, so-called hepatocyte nuclear factor 3β (HNF-3β) is an essential transcription factor for endoderm specification as well as hepatogenic fate. Similarly, ALB (hepatocyte-specific protein) and TDO2 (hepatocyte-specific enzyme, expressed by mature hepatocytes) were also detected by quantitative PCR at day 3 and their expression increased at day 6 of the induction system (Fig. 2a). The representative morphology of the ASC-derived hepatocyte-like cells of either a cancer patient's ASC or from the commercialized cells at the 13th day of induction is shown in Figure 2b. Importantly, 24 h of incubation with our new cocktail (Step II) alone is enough to dramatically influence the morphology of ASC (Donor #2) from fibroblast to epithelial (Fig. 3a). The pretreatment with Activin A and FGF4, however, is very important, because it induces the endodermal fate and alters further morphological changes and maturation of hepatocyte-like cells. As shown

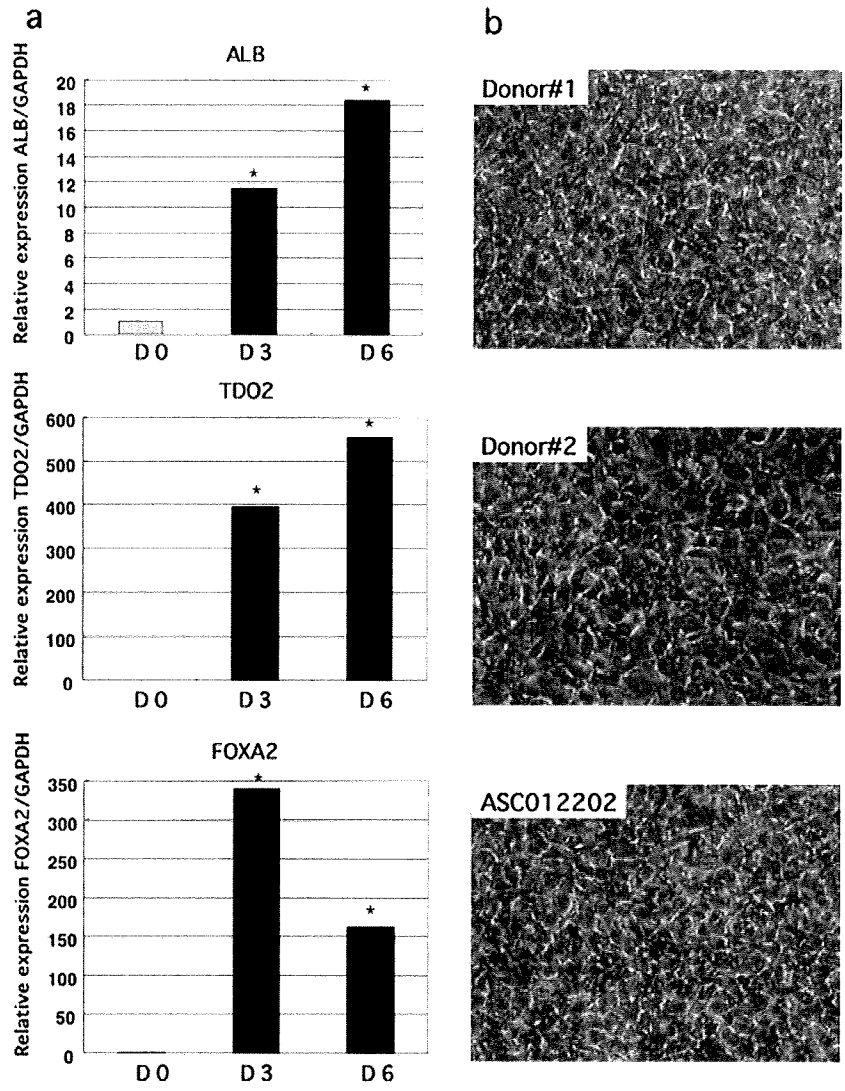

Figure 2 (a) Expression of albumin (ALB), tryptophan 2,3-dioxygenase (TDO2) and FOXA2 at day 3 (D3) (pretreatment with fibroblast growth factor [FGF]4 and Activin A) and day 6 (D6) (3 days of pretreatment with FGF4 and Activin A, and 3 days of treatment with hepatocyte growth factor [HGF], FGF1, FGF4, oncostatin M [OsM], dexamethasone [Dex], insulin-transferrin-selenium [ITS], dimethyl sulfoxide [DMSO], and nicotinamide) (■). Undifferentiated adipose-derived stem cells (ASC) (D0) (▨). Data were analyzed by the Pair Wise Fixed Reallocation Randomization Test©, $n = 3$. $^*P < 0.05$). (b) Morphological features of ASC-derived hepatocyte-like cells of ASC derived from Donor #1, Donor #2, and commercially available ASC012202.

in Figure 3(a), changes in the morphology of ASC-derived hepatocyte-like cells (Donor #2) at days 0, 4, 9 and 16 of hepatogenic induction indicate hepatocyte maturation. At day 13, ASC-derived hepatocyte-like cells expressed albumin (Fig. 3b), which was detected by immunostaining, using anti-human specific antibody. Undifferentiated ASC, however, did not express albumin (data not shown). We also checked the functionality of ASC-derived hepatocyte-like cells. Figure 3(c) represents the albumin production at days 3, 6 and 9 of the induction process. ASC-derived hepatocyte-like cells also revealed an ability to uptake low-density lipoprotein (LDL) and store glycogen (Fig. 4).

Transplantation of ASC-derived hepatocyte-like cells into mice with liver injury

To address whether ASC reveal therapeutic abilities to regenerate an injured liver, we transplanted ASC-derived hepatocyte-like cells of Donors #1 and #2 into nude mice with acute liver failure. CCl_4 injury generated oxidative stress and hepatocyte necrosis. Twenty-four hours after CCl_4 injection, mice revealed serious liver injury. Biochemical parameters such as ALT, AST, UA and ammonia were increased in mice with CCl_4 injury compared with non-injured mice (Fig. 5). We transplanted 1.5×10^6 cells of ASC-derived hepatocyte-like cells into a CCl_4-injured mouse. After transplantation, ALT and AST were significantly decreased to a value more than 50% lower than in non-transplanted and injured mice (Fig. 5). Likewise, ammonia concentration was significantly decreased after ASC-derived hepatocyte-like cell transplantation. UA, a marker of oxidative stress, was significantly decreased up to a normal level after transplantation of ASC-derived hepatocyte-like cells (Fig. 5). Hematoxylin-eosin staining revealed that the level of injury was the same in the injured, non-transplanted mice (Fig. 6b,e) as well as in the injured transplanted mice (Fig. 6c,f), in contrast to the non-injured non-transplanted mice (Fig. 6a,d). Significant morphological changes between those mice, however, were detected in the hepatocytes of the non-necrotic area. The

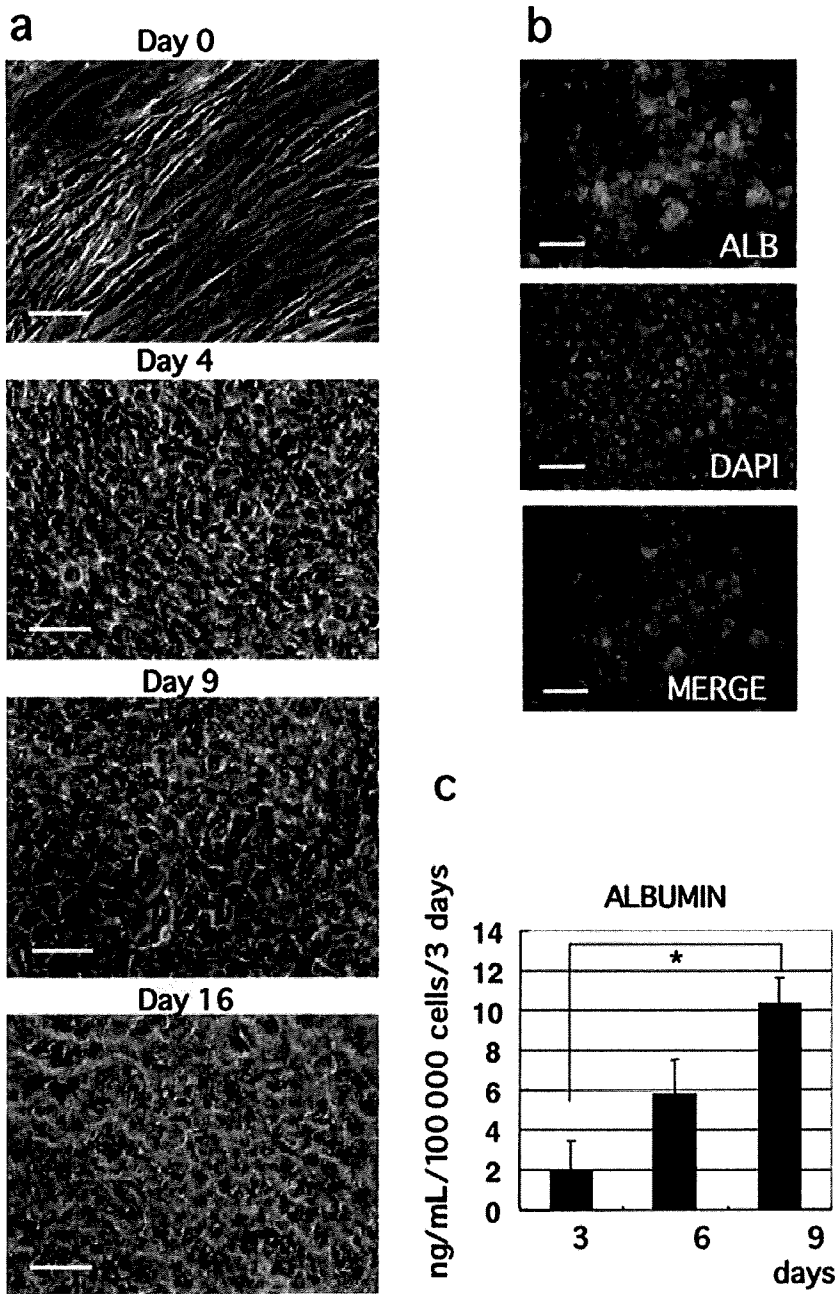

Figure 3 (a) Morphology of adipose-derived stem cells (ASC) (Donor #2) at days 0, 4, 9 and 16 during the hepatogenic induction process. (b) Albumin immunostaining analyses of ASC-derived hepatocyte-like cells at day 13 of induction. (c) Albumin production by ASC-derived hepatocyte-like cells at days 3, 6 and 9 of induction. Data are reported as the mean ± SD and were analyzed by Student's *t*-test, $n = 3$. $^*P < 0.05$). ALB, albumin; DAPI, 4,6-diamidino-2-phenylindole. Bar, 50 μm.

livers of injured, transplanted mice revealed less vacuolar degeneration caused by dilatation of mitochondria and rough endoplasmic reticulum. These observations reflect the data of the decrease of ALT and AST levels in injured transplanted mice. Therefore, transplantation of ASC-derived hepatocyte-like cells provided protection against CCl_4-induced hepatic injury. The above results indicate that ASC-derived hepatocyte-like cells generated within 13 days reveal hepatocyte-specific markers and functions *in vitro*, and improve liver function *in vivo*.

Discussion

Transplantation of hepatocytes generated from stem cells might become an easier, more efficient, and safer way than whole organ transplantation to cure patients suffering from liver disease. ASC can be very easily obtained with minimal invasiveness from a patient's own adipose tissue. Such a possibility sidesteps the obstacles regarding the risk of rejection, ethical issues, and availability of stem cells. We have already demonstrated mouse

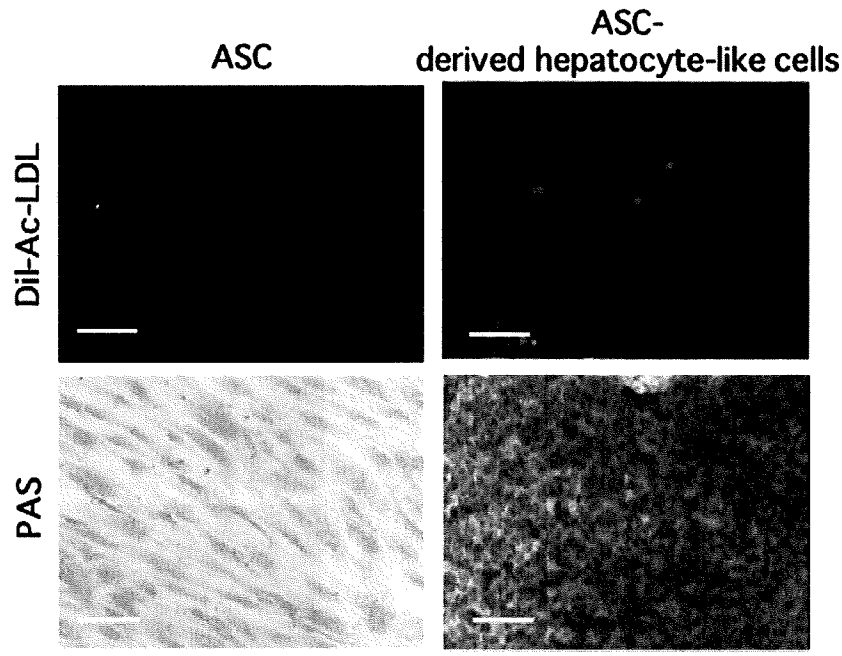

Figure 4 Low-density lipoprotein (LDL) uptake ability and glycogen storage ability (PAS) of adipose-derived stem cells (ASC)-derived hepatocyte-like cells at day 13 of induction. Dil-Ac-LDL, 1,1′-dioctade-cyl-3,3,3′,3′-tetramethyl-indocarbocyanine per-chlorate (Dil)-labeled acetylated LDL. Bar, 50 μm.

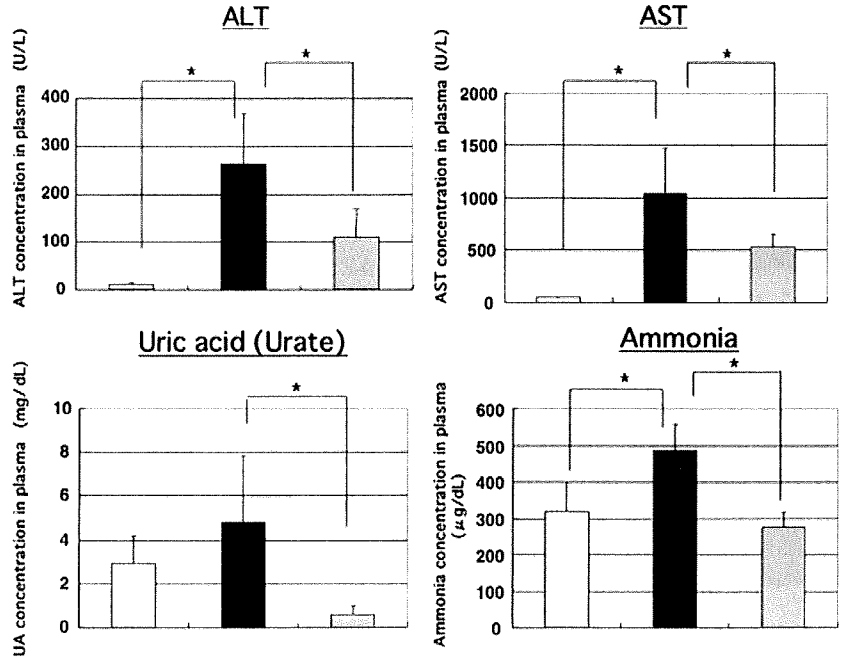

Figure 5 Biochemical analysis. Concentration of ammonia, alanine aminotransferase (ALT), aspartate aminotransferase (AST) and UA (uric acid/urate) in blood serum of killed mice. □, non-injured, non-transplanted mice; ■, injured and non-transplanted mice; ▨, injured and transplanted with adipose-derived stem cells (ASC)-derived hepatocyte-like cells (combined data of Donors #1 and #2). Data are presented as the mean ± SD and were analyzed by the Bonferroni correction $n = 3$. ($^*P < 0.05$).

embryonic stem cell[28–30] and human adult ASC[19] hepatogenic differentiation.

In the present study, we presented induction within a very short time of human ASC into hepatocyte-like cells. Thirteen days is sufficient to generate *in vitro* cells, which reveal hepatocyte-specific morphology, marker profile, and functionality. This is first time for such a short hepatogenic differentiation protocol to be presented. At the beginning we treated the cells with Activin A together with FGF4, which are important factors at early stages of endoderm formation in mouse liver development. Afterwards we used a number of factors essential for hepatogenic specification and hepatocyte morphology maintenance. We compared the hepatocyte-like cells obtained by a new rapid protocol with the hepatocyte-like cells of an original protocol,[19] and have found that they reveal all the analyzed functions, albeit much earlier. We observed that 24 h of *in vitro* cocktail treatment (HGF, FGF1,

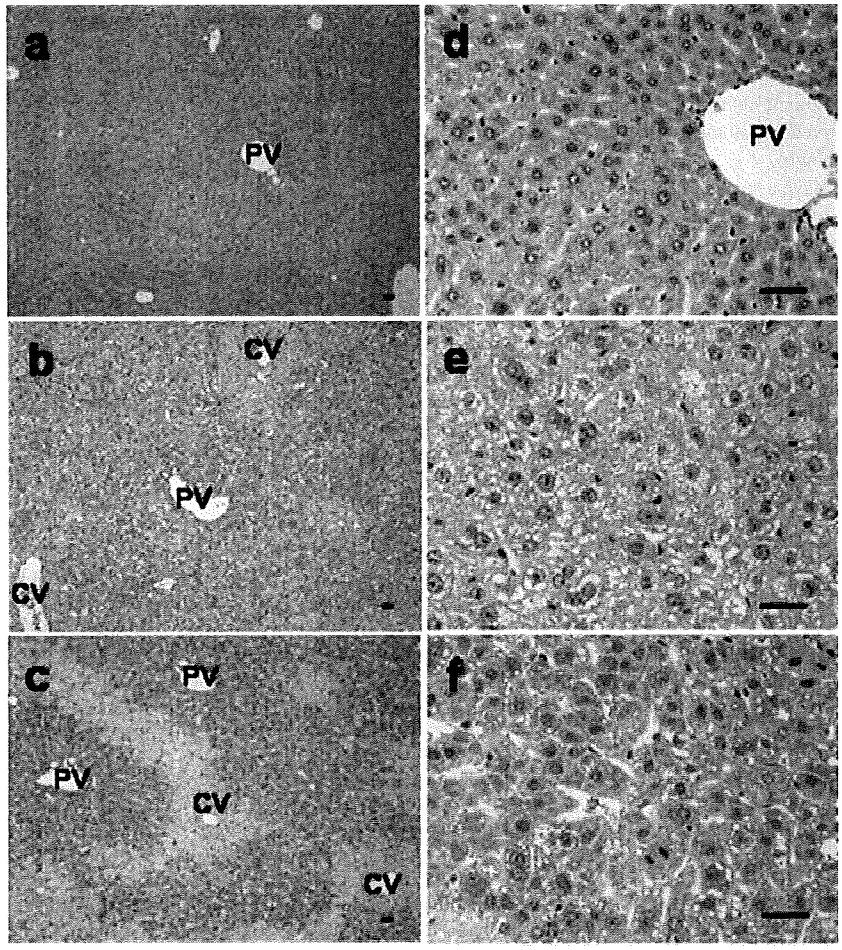

Figure 6 Hematoxylin-eosin staining of liver sections from (a,d) non-injured non-transplanted, (administered with olive oil and phosphate-buffered saline [PBS] [–]) mice ($n = 3$); (b,e) injured non-transplanted (administered with CCl_4 and PBS [–]) mice ($n = 3$); (c,f) injured transplanted (administered with CCl_4, 1 day after 1.5×10^6 ASC-derived hepatocyte-like cells transplantation) mice ($n = 4$). Panels a–c lower magnification 100 ×, panels d–f higher magnification 400 ×. CV, central vein; PV, portal vein. Scale bars represent 50 μm.

FGF4, OsM, Dex, ITS, nicotinamide, and DMSO) induces a dramatic change in morphology followed by little production of albumin at day 6 and a significant increase in the albumin level at day 9. However, using a previous protocol, albumin production was detected at days 30–50.

Prior to *in vivo* transplantation, it is important to induce hepatic fate within a short period of time and transplant the cells as fast as possible back into the patient with liver disease. Such a short period of time does not require large quantities of growth factors and may save much on expenses. Additionally, it will serve as hope and a great chance for a patient's total recovery. Significant morphological changes and albumin production as early as within 9 days suggest that it may be possible to even shorten the hepatic fate prior to transplantation. In the context of future clinical usage, a short period of stimulation to induce hepatic fate may be sufficient, because cells after transplantation may undergo further maturation in a regeneration environment.

Transplantation of *in vitro*-generated hepatocyte-like cells into CCl_4-injured nude mice resulted in the improvement of liver function *in vivo*. Interestingly, *in vivo* liver functions illustrated by the concentrations of ALT, AST, UA and ammonia were significantly decreased after ASC-derived hepatocyte-like cell transplantation (Fig. 5). The functional benefits of ASC-derived hepatocyte-like cell transplantation may be because of the functional support of the transplanted cells. It is still not clear by which mechanisms the transplanted cells improve the functioning of the liver. Fusion with host hepatocytes is not excluded. Likewise, the support and activation of endogenous progenitors are possible. Further studies examining the *in vivo* mechanism of homing, engraftment, and liver regeneration need to be conducted. It has been reported that in recipient liver, partial portal embolization, not partial portal ligation, improves engraftment of transplanted hepatocytes in a monkey primate preclinical model.[31] This provides new possibilities and strategies for future cell transplantation. It is essential to exclude any post-transplantation complications prior to any clinical trials. A long-term course experiment as well as safety issues should be carefully evaluated. Interestingly, in another study,[32] we observed that parameters such as ALT, AST, UA and ammonia were also decreased after undifferentiated ASC transplantation and we postulate that undifferentiated ASC per se compose a very attractive tool for the establishment of successful therapy for the liver.[32] We also speculate that the therapeutic potential of ASC may be due to the trophic activity of ASC.[32] These findings require additional studies with respect to safety issues post-

transplantation: however, they give great promise for future clinical applications.

Short-term hepatogenic induction methods may also have great usage in drug metabolism studies and toxicological analyses. In fact, we have already observed that ASC-derived hepatocyte-like cells reveal cytochrome activities (data not shown).

In conclusion, our study revealed that ASC have a special affinity towards hepatocyte differentiation *in vitro* and hepatocyte regeneration *in vivo*. Thus, ASC may be a superior choice for the establishment of therapy for an injured liver.

Acknowledgments

This work was supported in part by a Grant-in-Aid for the Third-Term Comprehensive 10-Year Strategy for Cancer Control; Health Science Research Grants for Research on the Human Genome and Regenerative Medicine from the Ministry of Health, Labor, and Welfare of Japan; and a Grant from Japan Health Sciences Foundation. We would like to thank Dr Shinobu Ueda, Ms Ayako Inoue and Ms Maho Kodama from the National Cancer Center Research Institute for their valuable advice and assistance.

References

1 Thomas MB, Zhu AX. Hepatocellular carcinoma: the need for progress. *J. Clin. Oncol.* 2005; **23**: 2892–99.
2 Pittenger MF, Mackay AM, Beck SC *et al.* Multilineage potential of adult human mesenchymal stem cells. *Science* 1999; **284**: 143–7.
3 Bieback K, Kern S, Kluter H, Eichler H. Critical parameters for the isolation of mesenchymal stem cells from umbilical cord blood. *Stem Cells* 2004; **22**: 625–34.
4 De Coppi P, Bartsch G Jr, Siddiqui MM *et al.* Isolation of amniotic stem cell lines with potential for therapy. *Nat. Biotechnol.* 2006; **25**: 100–6.
5 Shih DT, Lee DC, Chen SC *et al.* Isolation and characterization of neurogenic mesenchymal stem cells in human scalp tissue. *Stem Cells* 2005; **7**: 1012–20.
6 In't Anker PS, Scherjon SA, Kleijburg-van der Keur C *et al.* Isolation of mesenchymal stem cells of fetal or maternal origin from human placenta. *Stem Cells* 2004; **22**: 1338–45.
7 Zuk PA, Zhu M, Mizuno H *et al.* Multilineage cells from human adipose tissue: implications for cell-based therapies. *Tissue Eng.* 2001; **7**: 211–28.
8 Zuk PA, Zhu M, Ashjian P *et al.* Human adipose tissue is a source of multipotent stem cells. *Mol. Biol. Cell* 2002; **13**: 4279–95.
9 Schwartz RE, Reyes M, Koodie L *et al.* Multipotent adult progenitor cells from bone marrow differentiate into functional hepatocyte-like cells. *J. Clin. Invest.* 2002; **109**: 1291–302.
10 Sato Y, Araki H, Kato J *et al.* Human mesenchymal stem cells xenografted directly to rat liver are differentiated into human hepatocytes without fusion. *Blood* 2005; **106**: 756–63.
11 Ong SY, Dai H, Leong KW. Inducing hepatic differentiation of human mesenchymal stem cells in pellet culture. *Biomaterials* 2006; **27**: 4087–97.
12 Lange C, Bruns H, Kluth D, Zander AR, Fiegel HC. Hepatocytic differentiation of mesenchymal stem cells in cocultures with fetal liver cells. *World J. Gastroenterol.* 2006; **12**: 2394–7.
13 Lee KD, Kuo TK, Whang-Peng J *et al.* In vitro differentiation of human mesenchymal stem cells. *Hepatology* 2004; **40**: 1275–84.
14 Snykers S, Vanhaecke T, Papeleu P *et al.* Sequential exposure to cytokines reflecting embryogenesis: the key for in vitro differentiation of adult bone marrow stem cells into functional hepatocyte-like cells. *Toxicol. Sci.* 2006; **94**: 330–41.
15 Kang XQ, Zang WJ, Bao LJ *et al.* Fibroblast growth factor-4 and hepatocyte growth factor induce differentiation of human umbilical cord blood-derived mesenchymal stem cells into hepatocytes. *World J. Gastroenterol.* 2005; **11**: 7461–5.
16 Hong SH, Gang EJ, Jeong JA *et al.* In vitro differentiation of human umbilical cord blood-derived mesenchymal stem cells into hepatocyte-like cells. *Biochem. Biophys. Res. Commun.* 2005; **330**: 1153–61.
17 Seo MJ, Suh SY, Bae YC, Jung JS. Differentiation of human adipose stromal cells into hepatic lineage in vitro and in vivo. *Biochem. Biophys. Res. Commun.* 2005; **328**: 258–64.
18 Talens-Visconti R, Bonora A, Jover R *et al.* Hepatogenic differentiation of human mesenchymal stem cells from adipose tissue in comparison with bone marrow mesenchymal stem cells. *World J. Gastroenterol.* 2006; **12**: 5834–45.
19 Banas A, Teratani T, Yamamoto Y *et al.* Adipose tissue-derived mesenchymal stem cells as a source of human hepatocytes. *Hepatology* 2007; **46**: 219–28.
20 Bartholomew A, Sturgeon C, Siatskas M *et al.* Mesenchymal stem cells suppress lymphocyte proliferation in vitro and in vivo and prolong skin graft survival in vivo. *Exp. Hematol.* 2002; **30**: 42–8.
21 Di Nicola M, Carlo-Stella C, Magni M *et al.* Human bone marrow stromal cells suppress T-lymphocyte proliferation induced by cellular or nonspecific mitogenic stimuli. *Blood* 2002; **99**: 3838–43.
22 Tse WT, Pendleton JD, Beyer WM, Egalka MC, Guinan EC. Suppression of allogeneic T-cell proliferation by human marrow stromal cells: implications in transplantation. *Transplantation* 2003; **75**: 389–97.
23 Lazarus HM, Haynesworth SE, Gerson SL, Rosenthal NS, Caplan AI. Ex vivo expansion and subsequent infusion of human bone marrow-derived stromal progenitor cells (mesenchymal progenitor cells): implications for therapeutic use. *Bone Marrow Transplant.* 1995; **16**: 557–64.
24 Le Blanc K, Tammik L, Sundberg B, Haynesworth SE, Ringden O. Mesenchymal stem cells inhibit and stimulate mixed lymphocyte cultures and mitogenic responses independently of the major histocompatibility complex. *Scand. J. Immunol.* 2003; **57**: 11–20.
25 McIntosh K, Zvonic S, Garrett S *et al.* The immunogenicity of human adipose-derived cells: temporal changes in vitro. *Stem Cells* 2006; **24**: 1246–53.
26 Arnalich-Montiel F, Pastor S, Blazquez-Martinez A *et al.* Adipose-derived stem cells are a source for cell therapy of the corneal stroma. *Stem Cells* 2008; **26**: 570–9.
27 Cui L, Yin S, Liu W *et al.* Expanded adipose-derived stem cells suppress mixed lymphocyte reaction by secretion of prostaglandin E2. *Tissue Eng.* 2007; **13**: 1185–95.
28 Teratani T, Yamamoto H, Aoyagi K *et al.* Direct hepatic fate specification from mouse embryonic stem cells. *Hepatology* 2005; **41**: 836–46.
29 Yamamoto Y, Teratani T, Yamamoto H *et al.* Recapitulation of in vivo gene expression during hepatic differentiation from embryonic stem cells. *Hepatology* 2005; **42**: 558–67.
30 Yamamoto H, Quinn Q, Asari A *et al.* Differentiation of embryonic stem cells into hepatocytes: biological functions and therapeutic application. *Hepatology* 2003; **37**: 983–93.
31 Dagher I, Boudechiche L, Branger J *et al.* Efficient hepatocyte engraftment in a nonhuman primate model after partial portal vein embolization. *Transplantation* 2006; **82**: 1067–73.
32 Banas A, Teratani T, Yamamoto Y *et al.* In vivo therapeutic potential of human adipose tissue-derived mesenchymal stem cells (ASCs), after transplantation into mice with liver injury. *Stem Cells* 2008; (in press).

JOURNAL OF VIROLOGY, July 2009, p. 6922–6928 Vol. 83, No. 13
0022-538X/09/$08.00+0 doi:10.1128/JVI.02674-08

Genetic Analysis of Hepatitis C Virus with Defective Genome and Its Infectivity in Vitro▽

Kazuo Sugiyama,[1]* Kenji Suzuki,[2] Takahide Nakazawa,[3] Kenji Funami,[1] Takayuki Hishiki,[4] Kazuya Ogawa,[4] Satoru Saito,[5] Kumiko W. Shimotohno,[2] Takeshi Suzuki,[2] Yuko Shimizu,[1] Reiri Tobita,[6] Makoto Hijikata,[7] Hiroshi Takaku,[6] and Kunitada Shimotohno[1,4]

Center for Integrated Medical Research, Keio University, Shinjuku-ku, Shinanomachi 35, Tokyo 160-8582, Japan[1]; Division of Basic Biological Sciences, Faculty of Pharmacy, Keio University, Tokyo 105-8512, Japan[2]; Department of Gastroenterology, Internal Medicine, Kitasato University East Hospital, Kanagawa 228-8520, Japan[3]; Research Institute, Chiba Institute of Technology, Chiba 275-0016, Japan[4]; Yokohama City University Hospital, Kanagawa 236-0004, Japan[5]; Department of Life and Environmental Sciences, Chiba Institute of Technology, Chiba 275-0016, Japan[6]; and Institute for Virus Research, Kyoto University, Kyoto 606-8507, Japan[7]

Received 29 December 2008/Accepted 6 April 2009

Replication and infectivity of hepatitis C virus (HCV) with a defective genome is ambiguous. We molecularly cloned 38 HCV isolates with defective genomes from 18 patient sera. The structural regions were widely deleted, with the 5′ untranslated, core, and NS3-NS5B regions preserved. All of the deletions were in frame, indicating that they are translatable to the authentic terminus. Phylogenetic analyses showed self-replication of the defective genomes independent of full genomes. We generated a defective genome of chimeric HCV to mimic the defective isolate in the serum. By using this, we demonstrated for the first time that the defective genome, as it is circulating in the blood, can be encapsidated as an infectious particle by *trans* complementation of the structural proteins.

Viruses with a deletion mutation in their genome have been identified as defective interfering (DI) particles for many virus species (1, 3, 9, 16). Part of the DI virus genome is deleted, but regions indispensable for replication and packaging are preserved. Most DI viruses occur spontaneously in the course of cell culture infected with a high titer of wild-type viruses. Hepatitis C virus (HCV) with a defective genome has been found in liver and serum specimens of some HCV patients (4, 8, 15). HCV has a plus-strand RNA genome that encodes the viral core, E1, E2, and p7 structural proteins and NS2, NS3, NS4A, NS4B, NS5A, and NS5B nonstructural proteins (10). According to the reports, the deletions have been found mainly in the structural region and most of the deletions are in frame, but some deletions are out of frame (4), raising questions about whether the defective HCV genome is merely a by-product of a full genome or a self-replicating genome and whether it can be encapsidated into an infectious virus particle.

In the present study, we molecularly cloned 38 HCV isolates with defective genomes from HCV patient sera to address these questions by genetic analyses and infection experiments. As long as we explored, all of the deletions were in frame, indicating the potential to support translation from the authentic initiation codon to the termination codon, although the structural region was widely deleted, as reported previously. Phylogenetic analyses evidenced self-replication of the defective genomes independent of full genomes. We demonstrated for the first time, by *trans* complementation experiments, that the defective genome, as it is circulating in the blood, can be encapsidated as an infectious particle, designated HCV_{CCD}.

First, to amplify HCV cDNAs in 21 serum specimens from 18 HCV patients (genotype 1b), we performed three sets of long-distance reverse transcription (RT)-PCRs flanking (i) the 5′ untranslated region (UTR) to the 5′ part of the NS3 region, (ii) the remaining part of the NS3 region to the end of NS5B, and (iii) the 5′ UTR to the end of the NS5B region (Fig. 1A). The specimens were collected with informed consent. cDNA was synthesized with RNase H-deficient reverse transcriptase Superscript III (Invitrogen, Carlsbad, CA) at a higher temperature (55°C) to reduce template switching and mispriming. PCRs were performed in a (hemi)nested manner with high-fidelity polymerase KOD plus or KOD FX (Toyobo, Osaka, Japan) as described previously (5). For some target nucleotide positions, a mixture of two or three primers was used to reduce mismatches due to sequence heterogeneity (Table 1). Of the 21 specimens examined, representative results are shown in Fig. 1. An amplicon of the 5′ UTR-NS3 region of the predicted size (ca. 3.7 kb) was detected in all specimens (18/18), and representative results are shown in Fig. 1B. In addition, a shorter amplicon suggestive of a defective HCV genome was simultaneously present in four specimens from 1 (R4) of 12 cases of clinically mild hepatitis and from 3 (T5, K3, and K4-pre) of 6 cases of active hepatitis (clinical data not shown). Defective genomes were found in the patients with relatively higher copy numbers of HCV RNA ($>8.1 \times 10^5$ copies/ml in the 5′ UTR, Table 2), suggesting that the coexistence of a defective genome is related to hepatitis severity. The authentic-size amplicon was poorly detected when coexisting with a defective HCV genome shorter than 2 kb (T5 and K3), presumably because of preferential amplification of the shorter amplicon. A shorter amplicon was not detected for the NS3-

* Corresponding author. Mailing address: Center for Integrated Medical Research, Keio University, Shinjuku-ku, Shinanomachi 35, Tokyo 160-8582, Japan. Phone: 81-3-3353-1211. Fax: 81-47-478-0527. E-mail: sygiyamkz@a8.keio.jp.

▽ Published ahead of print on 15 April 2009.

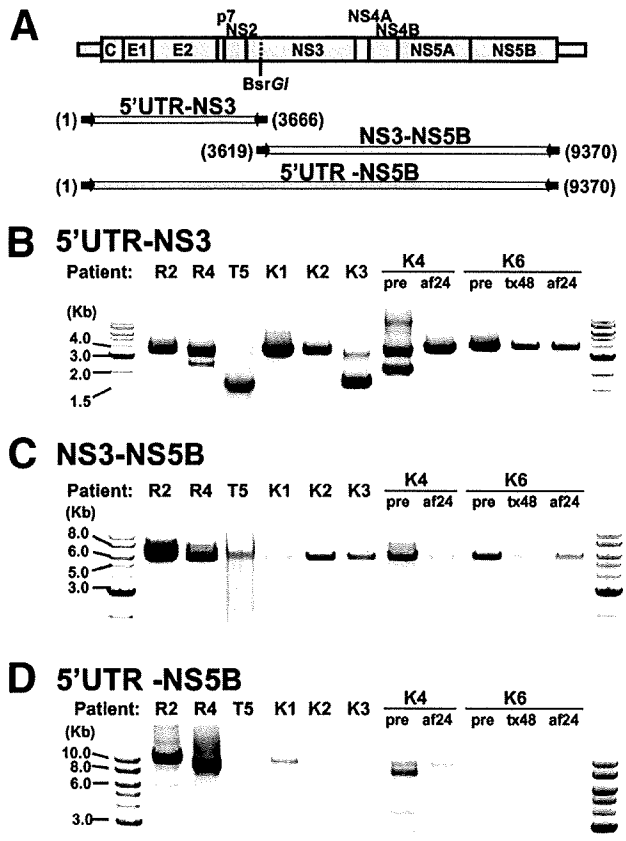

FIG. 1. Representative results of long-distance RT-PCRs for serum HCV. (A) The three sets of long-distance RT-PCR used: 5′ UTR-NS3 (5′ UTR to the 5′ part of the NS3 region), NS3-NS5B (the remaining part of the NS3 region to the end of NS5B), and 5′ UTR-NS5B (5′ UTR to the end of the NS5B region). The nucleotide positions of the 5′ and 3′ ends of each amplicon are indicated in parentheses. PCR products were electrophoresed and stained with ethidium bromide. Results of the representative 11 specimens (eight patients) are shown for 5′ UTR-NS3 (B), NS3-NS5B (C), and 5′ UTR-NS5B (D). Serum specimens were collected from patients K4 and K6 before interferon treatment (pre), at the end of the full 48-week treatment period (tx48), and 24 weeks after the full treatment period (af24). DNA molecular size markers are at both sides of panels B to D.

NS5B region, while the amplicon of the predicted size (ca. 5.6 kb) was detected in all of the specimens, albeit with various efficiencies (Fig. 1C). The 5′ UTR-NS5B region, which covers almost the whole genome, was then amplified, and an amplicon of the predicted size (9.4 kb) was detected in 10 specimens from nine patients (5 specimens in Fig. 1D). Of the successfully amplified specimens, two (R4 and K4-pre) also contained a shorter amplicon, in accordance with the results of the 5′ UTR-NS3 PCR. The NS3-NS5B region is essential for autonomous replication of HCV as an RNA replicon in vitro (5–7). It has been shown that NS5A is the only nonstructural protein that can *trans* complement HCV replication (13). They used a nonadaptive mutation of NS5A as a replication-incompetent NS5A protein instead of a deletion mutant protein. Thus, we speculate that deletion of the NS3-NS5B region cannot be complemented in *trans*. Intriguingly, the shorter amplicon was not detected after full-term interferon treatment in patient K4 (K4-af24), although it was detected prior to treatment (K4-pre) (Fig. 1B and D). The possible reasons for this are that (i) the defective genome disappeared naturally, (ii) packaging of the defective genome by the helper virus was impeded by an unknown mechanism of interferon, or (iii) replication of the defective genome is preferentially inhibited by the interferon pathway. Further studies are needed to reveal the effect of a defective HCV genome on the pathogenesis and treatment of HCV.

A total of 38 isolates with defective HCV genomes were molecularly cloned into plasmid vector pASGT (unpublished data) from the shorter amplicons of the 5′ UTR-NS3 PCR from four serum specimens (R4, T5, K3, and K4-pre in Fig. 1B) at the AscI and BsrGI restriction sites. The nucleotide sequences were determined with an autosequencer (3730 DNA analyzer; Applied Biosystems, Foster City, CA). Sequence analyses revealed that the structural region was widely deleted in all of the defective isolates and that the deletion ranges were quite diverse among the isolates (extending up to the NS2 region) (Fig. 2A). In contrast, the 5′ UTR and core regions were constantly preserved, suggesting that these regions, as well as the NS3-NS5B region, are indispensable for the production of HCV with a defective genome. Intriguingly, defective genomes with different deletion patterns coexisted in single specimens from two patients (three patterns in patient K3 and four patterns in patient K4-pre). Moreover, two deletions in a single genome were observed in five isolates from patient R4 (isolate R4S-5). As many as three deletions in a single genome were observed in the isolate from patient K3 (e.g., isolate K3S-15), in which two small deletions resulted in two tiny residual fragments. Such diversity in deletion ranges indicates flexibility of the remaining structural region for the replication of defective HCV genomes. Nevertheless, all of the deletions identified in the 38 isolates were in frame (Fig. 2B), implying that these defective HCV genomes have the potential for translation from the core to the authentic end of NS5B without a frameshift.

To determine the ratio of defective to full genomes, we performed quantitative PCRs targeting a relatively conserved E2 sequence, which is commonly deleted in the defective genomes, with primers listed in Table 1. Calculation of the 5′ UTR/E2 ratio, which must theoretically be 1 without the existence of the defective genome, showed higher values (1.7 to 2.45) in specimens containing the defective genomes (R4, K3, and K4pre in Table 2), indicating that the defective genome level in serum is 0.7 to 1.45 times the full genome level. However, to clarify the impact of defective genomes on pathogenesis and their effect on the treatment of HCV, accumulation of more data is needed.

The nucleotide sequence comparison of 38 defective HCV isolates showed sequence diversity. Such diversity was observed even among isolates obtained from the same specimen. Perhaps such diversity is a result of self-replication and the subsequent evolution of the defective HCV genome. To explore this possibility, phylogenetic analyses were performed on the nucleotide sequence data from patient K4. Sequences at the 5′ and 3′ maximum overlapping regions located outside the deletions were separately compared (Fig. 2A), and phylogenetic trees were created by the neighbor-joining method with GENETYX software (Genetyx Inc., Tokyo, Japan). As a re-

TABLE 1. Primers used for long-distance and quantitative RT-PCRs in this study

Test and region(s)	Direction	Primer(s)[a]	Sequence[b]	Position[c]
Long-distance PCR				
5′ UTR-NS3	RT	606R/712R	GTTTCCATAGACTC(A/G)ACGGG	3930–3949
5′ UTR-NS3, 5′ UTR-NS5B	1st forward	420	GGCGACACTCCACCATAGATCACTC	1–42
5′ UTR-NS3	1st reverse	605R/713R	ACCGGAATGACATCAGCATG(T/C)CTCGT	3741–3766
5′ UTR-NS3, 5′ UTR-NS5B	2nd forward	AscT7-420	ATCGTAGGCGCGCCT*CTAATACGACTCACTATA*GC CAGCCCCCGATTGGGGGCGACACTCCACCATAGATCACTC	1–42
5′ UTR-NS3	2nd reverse	604R/714R	CGAGGTCCTGGTCTACATT(G/A)GTGTACAT	3639–3666
NS3-NS5B, 5′ UTR-NS5B	RT	386R	AATGGCCTATTGGCCTGGAG	9390–9392
NS3-NS5B	1st forward	602/723	CCACCGCAACACAATCTTTCCT(G/A)GCGAC	3529–3556
NS3-NS5B, 5′ UTR-NS5B	1st reverse	719R/720R/721R	GAGTGTTTAGCTCCCCGTTCA(T/C/G)CGGTTGGG	9363–9392
NS3-NS5B	2nd forward	603/724	CAAAGGGTCCAATCACCCA(A/G)ATGTACAC	3619–3646
NS3-NS5B, 5′ UTR-NS5B	2nd reverse	607R/654R/722R	CGGTTGGGGAGCAGGTA(G/A/G)A(T/T/C)GCCTAC	9345–9370
Quantitative PCR				
5′ UTR	RT	738RH	ACTCGCAAGCACCCTATCAGGC	291–312
5′ UTR	Forward	736	AAGCGTCTAGCCATGGCGTTAGTA	73–96
5′ UTR	Reverse	737R	GGCAGTACCACAAGGCCTTTCG	272–293
5′ UTR	Probe	733FB	FAM-TCTGCGGAACCGGTGAGTACAC-BHQ1	147–168
E2	RT	743RH/744RH/753RH/753RH	CAACGCTCTCCTCG(A/A/G/G)GTCCA(A/G/A/G)TTGCA	2271–2296
E2	Forward[d]	751/752	GGCCTCCACATGGCAA(C/T)TGGTTCGG	1972–1993
E2	Forward[d]	739/740	CCGCCGCAAGGCAACTGGTT(C/T)GG	1974–1993
E2	Reverse	741R/742R	GCCTCGGGGTGCTTCCGGAAGCA(G/A)TCCGT	2088–2116
E2	Probe	734FB/735FB	FAM-TGGATGAA(T/C)AGCACTGGGTTCACCAAGAC-BHQ1	2001–2029

[a] Primers separated by slashes harbor a nucleotide substitution(s) (in parentheses) in the sequence in the same order.
[b] An underline and a double underline indicate recognition sequences for AscI and BsrGI, respectively, with which the PCR products were subcloned into plasmid vector pASGT5. Italics denote the T7 promoter, which was used to synthesize RNA in vitro from the T5S2 isolate (Fig. 4A).
[c] Nucleotide positions correspond to the HCV-JS sequence (12).
[d] Forward primers for E2 were mixed in the reaction mixture.

sult, isolates with the same deletion pattern formed genetic clusters that were distinct from each other, as well as from those of nondefective HCV isolates (Fig. 3A and B). Similar results were obtained for the other patients with defective HCV genomes (data not shown). These results suggest that a defective HCV genome is capable of replication to accumulate mutations and to evolve independently of the nondefective HCV genome.

TABLE 2. Quantitative PCRs for the 5′ UTR and E2 regions of HCV[a]

Region for quantification	No. of copies/ml		5′ UTR/E2 ratio
	5′ UTR	E2	
R2	2.0×10^6	1.7×10^6	1.17
R4	5.3×10^6	2.2×10^6	2.44
T5	ND[b]	ND[b]	
K1	8.3×10^5	8.4×10^5	0.99
K2	3.6×10^5	3.5×10^5	1.01
K3	8.6×10^5	5.1×10^5	1.7
K4pre	8.1×10^5	3.3×10^5	2.45
K4af24	4.5×10^5	4.4×10^5	1.01

[a] For quantification of the 5′ UTR and E2 regions, the TaqMan Fast PCR Universal mixture and the 7500 Fast Real-Time PCR system (Applied Biosystems) were used in a two-step method with the primers and probes shown in Table 1 according to the manufacturer's protocol. The copy number of HCV was determined by the standard-curve method with serial dilutions of the synthesized full-length HCV RNA.
[b] ND, not determined due to sample shortage.

Next, the ability of the defective HCV genome to be encapsidated and released from cells as HCV_{CCD} was examined. A genotype 1b replicon RNA lacking the structural region was synthesized by using defective isolate T5S-2 from patient T5 (Fig. 2 and 4A) as the template in an in vitro transcription system (MEGAscript T7 kit; Ambion, Inc., Austin, TX) under the control of the T7 promoter. Also, capped mRNA encoding the genotype 1b structural proteins from the same patient (designated C-NS2 in Fig. 4A) was synthesized in vitro with the mMessage mMachine T7 kit (Ambion). Both synthesized RNAs were cotransfected into Huh7.5 hepatoma cells. However, HCV_{CCD} was not obtained, presumably because of low replication or virus productivity of genotype 1b HCV per se. In fact, we transfected the defective RNA alone and observed the replication and protein expression of HCV, but with low efficiency (data not shown). Thus, to augment virus productivity, a JFH1-based chimeric HCV genome (genotype 1b/2a) and its deletion mutant were generated to mimic isolate T5S-2 (designated TNS2J1 and TNS2J1ΔS, respectively, Fig. 4A). JFH1 is genotype 2a HCV isolate that can produce high levels of infectious virus (14). To verify the virus productivity of TNS2J1, Huh7.5 cells (10-cm plate) were transfected with 10 μg of in vitro-synthesized RNA from TNS2J1 or JFH1 by lipofection with TransMessenger transfection reagent (Qiagen, Valencia, CA) according to the manufacturer's protocol. Two days later, the culture medium was concentrated 10-fold and inoculated into naïve Huh7.5 cells (four-well chamber

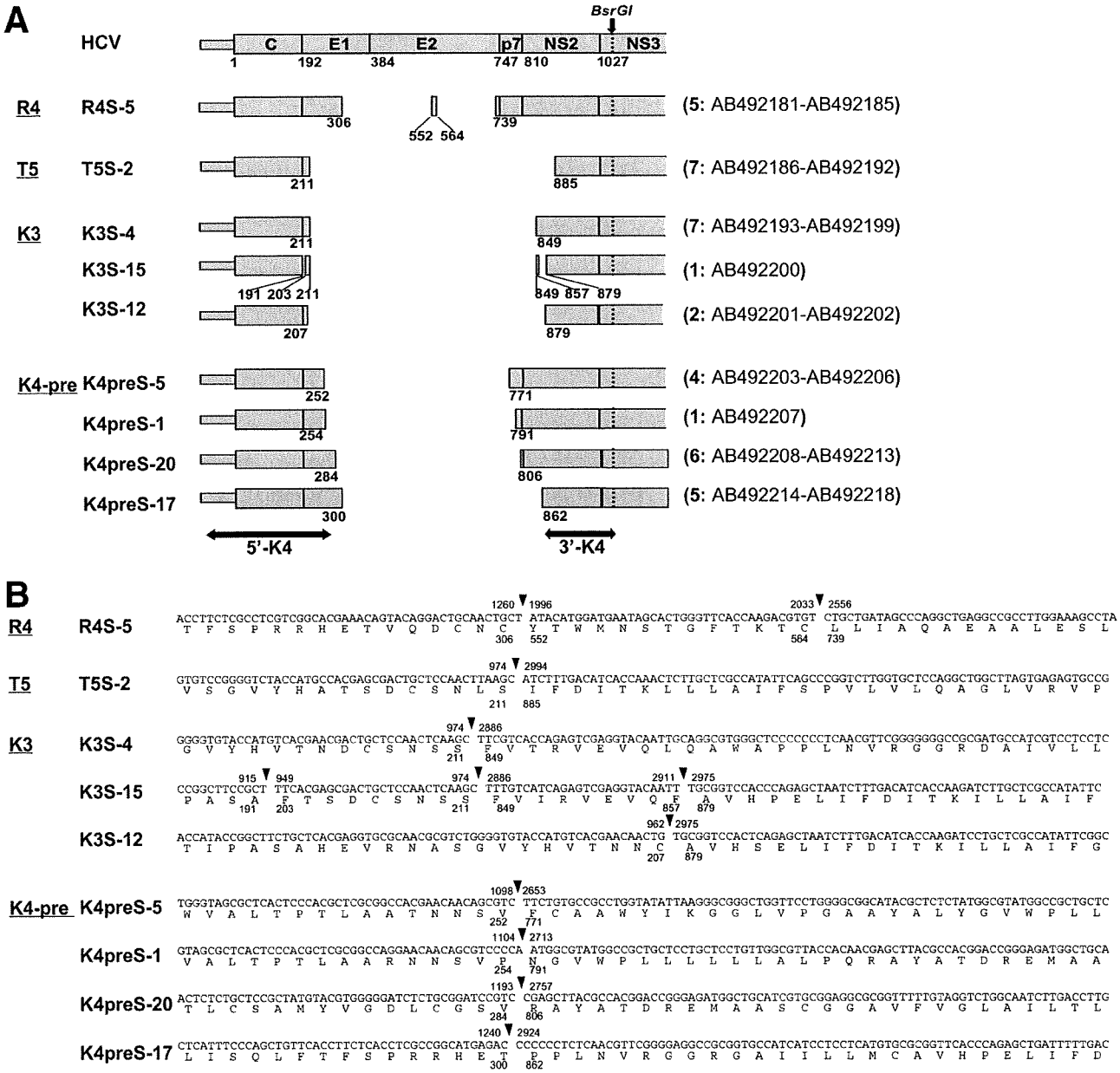

FIG. 2. Sequence analysis of the defective HCV genomes. A total of 38 isolates were molecularly cloned into a plasmid vector and sequenced. Data from representative isolates are presented. Nucleotide positions and deduced amino acid positions correspond to those of genotype 1b strain HCV-JS (12). (A) Defects located in the structural region were compared. The remaining regions are illustrated as shaded boxes. Below the boxes are numbers indicating amino acid positions at the end of each remaining region. At the top of the panel is the HCV genome with the amino acid position at the N terminus of each HCV protein below. The BsrGI restriction site that was used to clone the PCR products is shown as a dotted line. Each value in parentheses at the right is the number of isolates showing the same deletion pattern, followed by the GenBank accession number(s). The two-headed arrows indicate the 5′ and 3′ maximum overlapping regions among the defective HCV isolates in the K4-pre specimen that are compared in the following phylogenetic analyses (5′-K4 and 3′-K4; see Fig. 3). (B) Deletion breakpoints and their adjacent nucleotides and deduced amino acid sequences are indicated. Solid triangles denote breakpoints, and numbers indicate the nucleotide positions (above) and amino acid positions (below) at the junctions.

slide). Cells inoculated with the culture medium from TNS2J1 RNA-transfected cells markedly expressed HCV protein, as shown by immunofluorescent staining (Fig. 4B). The percentage of HCV-positive cells in chimera-infected cells, 40% (565/1,240), was greater than that of JFH1, 3% (37/1,210), demonstrating that the chimeric genome TNS2J1 can produce infectious HCV more robustly than JFH1 can ($P < 0.0001$).

Taking advantage of this chimeric genome, we conducted *trans* complementation experiments. To mimic the T5S-2 iso-

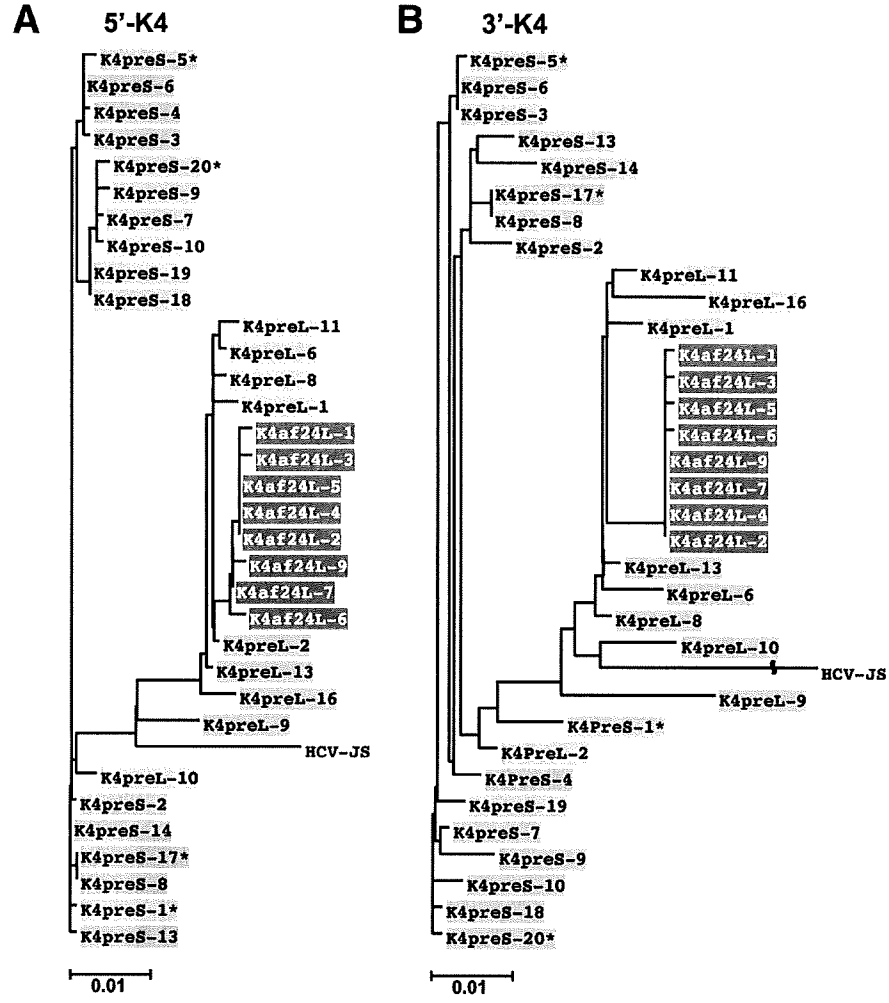

FIG. 3. Phylogenetic analyses of defective HCV genomes. Nucleotide sequence data from 33 isolates from patient K4 were used for phylogenetic analyses. The defective HCV genome (16 isolates) and the nondefective HCV genome coexisting before interferon treatment (9 isolates; GenBank accession no. AB492219 to AB492227) and those after treatment (8 isolates; GenBank accession no. AB492228 to AB492235) were compared in the 5′ and 3′ maximum overlapping regions separately (5′-K4 and 3′-K4 in Fig. 2A). Phylogenetic trees were created for the respective regions (A and B). In the isolate designations, pre and af24 stand for before and after interferon treatment and S and L stand for defective and nondefective HCV genomes, respectively. Isolates with the same deletion pattern (according to K4-pre in Fig. 2) are shaded in the same color. Asterisks denote the representative isolates illustrated in Fig. 2.

late, the region corresponding to the defect found in T5S-2 was identically deleted from the TNS2J1 genome (designated TN2J1ΔS, Fig. 4A). Ten micrograms of synthesized RNA of TN2J1ΔS was cotransfected into Huh7.5 cells (10-cm plate) together with 10 μg of synthesized capped mRNA encoding the structural region, including part of the nonstructural region of TNS2J1, designated C-NS2 or C-NS3P (Fig. 4A). Two days later, the culture medium was concentrated and inoculated into naïve Huh7.5 cells as previously described. HCV protein was expressed when cells were inoculated with the medium of cells cotransfected with TN2J1ΔS RNA and C-NS2 or C-NS3P mRNA, whereas no expression was observed in the case of TN2J1ΔS RNA alone (Fig. 4C). To stably provide the structural proteins in *trans*, packaging cell lines were established by retroviral transduction (2) of Huh7.5 cells with genes encoding the C-NS2 or C-NS3P region (Fig. 4A). These packaging cell lines were transfected with TN2J1ΔS RNA, and HCV protein was expressed in cells inoculated with the culture medium from the RNA-transfected packaging cells (Fig. 4D). Notably, the construct C-NS2 helped to produce HCV_{CCD} more efficiently than C-NS3P did (Fig. 4C). We observed less expression of the structural proteins with the C-NS3 construct than with the C-NS2 construct in a transient expression experiment (data not shown). One possible reason for this is that the C-NS3 construct needs one additional process, i.e., cleavage between NS2 and NS3, to produce NS2 and may affect the other proteins. Otherwise, it is simply because of the difference in the lengths of the constructs. These results indicate that a defective HCV genome lacking the structural region can be encapsidated by *trans* complementation of the structural proteins, thus conferring infectivity in vivo. Recently, a *trans*-packaging system consisting of an HCV subgenomic replicon and a reporter gene

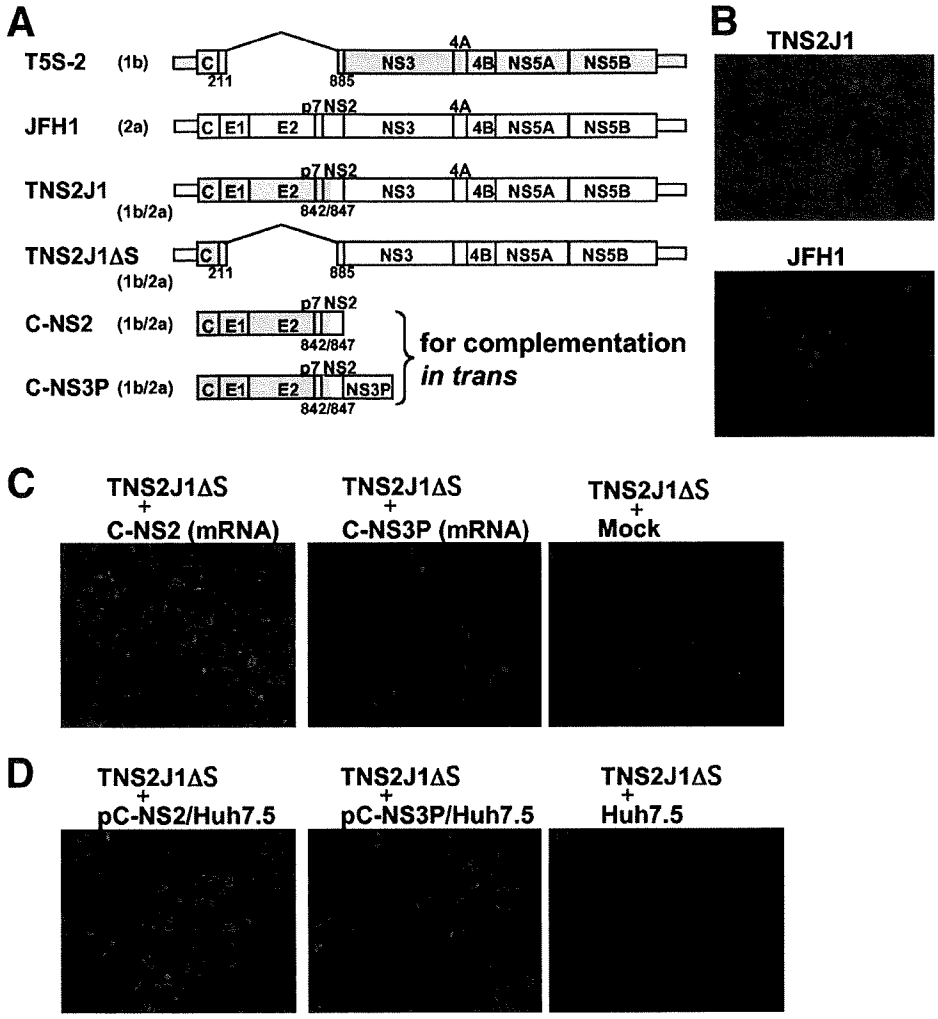

FIG. 4. In vitro infectivity of deletion mutant of chimeric HCV conferred by *trans* complementation of structural proteins. (A) Schematics of the following HCV genomic constructs: the defective HCV isolate (T5S-2), JFH1, chimeric virus of genotypes 1b and 2a (TNS2J1), and its deletion mutant (TNS2J1ΔS). C-NS2 and C-NS3 are fragments encoding the region from the core to the C terminus of the NS2 region and to the C terminus of the serine protease moiety in NS3, respectively. For the *trans* complementation experiments, the latter two constructs were inserted into pcDNA3.1 (Invitrogen) to synthesize capped mRNAs or into retroviral vector pCX4bsr (GenBank accession no. AB086384) to establish packaging cell lines stably expressing the proteins. Shaded and open boxes represent genotypes 1b (isolate from patient T5) and 2a (JFH1), respectively. The numbers below the boxes are amino acid positions at deletion breakpoints or at PCR-based recombination junctions. Naïve Huh7.5 cells were inoculated with the culture medium from cells transfected with JFH1 or TNS2J1 RNA (B), from cells cotransfected with TNS2J1ΔS RNA together with the structural region mRNA (C-NS2 or C-NS3P) or TNS2J1ΔS RNA alone (C), and from the packaging cell line (C-NS2/Huh7.5 or C-NS3P/Huh7.5) transfected with TNS2J1ΔS RNA and parental Huh7.5 cells transfected with TNS2J1ΔS RNA (D). HCV protein was detected by human HCV serum (1:500) by the indirect immunofluorescent method with Alexa Fluor 568 goat anti-human immunoglobulin G (1:200; red; Invitrogen). Nuclei were counterstained with 4′,6′-diamidino-2-phenylindole (DAPI; blue).

was also reported in which an intragenotypic chimera (2a/2a) was used as the most efficient packaging construct (11). Our packaging system used an efficient intergenotypic chimera (1b/2a) to encapsidate a genome mimicking a naturally occurring deletion (1b). Thus, although its efficiency may be different, our system could be a useful tool for the study of HCV_{CCD} of chimeric genome 1b/2a or genotype 1b.

Taken together, genetic analyses of the defective HCV genome showed the potential of its translation and self-replication. These defective genomes can be encapsidated into infectious virus-like particles by *trans* complementation of the structural proteins in vitro. The 5′ UTR and core regions, which are preserved in defective HCV genomes, are targets for the clinical quantification of HCV. Therefore, measured values may represent additive values for defective and nondefective HCVs and the method used for HCV quantification should be reevaluated.

We thank H. Kato, R. Shiina, and H. Yamamoto for technical assistance; T. Wakita for the gift of JFH1; C. Rice for the gift of Huh7.5 cells; and T. Akagi for the gift of retroviral vector pCX4bsr.

This work was supported by a grant-in-aid for scientific research (C) from the Japan Society for the Promotion of Science (KAKENHI18590454) and a grant-in-aid for research on hepatitis from the Ministry of Health, Labor, and Welfare.

REFERENCES

1. **Brinton, M. A.** 1983. Analysis of extracellular West Nile virus particles produced by cell cultures from genetically resistant and susceptible mice indicates enhanced amplification of defective interfering particles by resistant cultures. J. Virol. **46**:860–870.
2. **Chen, C. J., K. Sugiyama, H. Kubo, C. Huang, and S. Makino.** 2004. Murine coronavirus nonstructural protein p28 arrests cell cycle in G_0/G_1 phase. J. Virol. **78**:10410–10419.
3. **Huang, A. S., and D. Baltimore.** 1970. Defective viral particles and viral disease processes. Nature **226**:325–327.
4. **Iwai, A., H. Marusawa, Y. Takada, H. Egawa, K. Ikeda, M. Nabeshima, S. Uemoto, and T. Chiba.** 2006. Identification of novel defective HCV clones in liver transplant recipients with recurrent HCV infection. J. Viral Hepat. **13**:523–531.
5. **Kato, N., K. Sugiyama, K. Namba, H. Dansako, T. Nakamura, M. Takami, K. Naka, A. Nozaki, and K. Shimotohno.** 2003. Establishment of a hepatitis C virus subgenomic replicon derived from human hepatocytes infected in vitro. Biochem. Biophys. Res. Commun. **306**:756–766.
6. **Kishine, H., K. Sugiyama, M. Hijikata, N. Kato, H. Takahashi, T. Noshi, Y. Nio, M. Hosaka, Y. Miyanari, and K. Shimotohno.** 2002. Subgenomic replicon derived from a cell line infected with the hepatitis C virus. Biochem. Biophys. Res. Commun. **293**:993–999.
7. **Lohmann, V., F. Körner, J. Koch, U. Herian, L. Theilmann, and R. Bartenschlager.** 1999. Replication of subgenomic hepatitis C virus RNAs in a hepatoma cell line. Science **285**:110–113.
8. **Noppornpanth, S., S. L. Smits, T. X. Lien, Y. Poovorawan, A. D. Osterhaus, and B. L. Haagmans.** 2007. Characterization of hepatitis C virus deletion mutants circulating in chronically infected patients. J. Virol. **81**:12496–12503.
9. **Poidinger, M., R. J. Coelen, and J. S. Mackenzie.** 1991. Persistent infection of Vero cells by the flavivirus Murray Valley encephalitis virus. J. Gen. Virol. **72**(Pt. 3):573–578.
10. **Shimotohno, K.** 1995. Hepatitis C virus as a causative agent of hepatocellular carcinoma. Intervirology **38**:162–169.
11. **Steinmann, E., C. Brohm, S. Kallis, R. Bartenschlager, and T. Pietschmann.** 2008. Efficient *trans*-encapsidation of hepatitis C virus RNAs into infectious virus-like particles. J. Virol. **82**:7034–7046.
12. **Sugiyama, K., N. Kato, T. Mizutani, M. Ikeda, T. Tanaka, and K. Shimotohno.** 1997. Genetic analysis of the hepatitis C virus (HCV) genome from HCV-infected human T cells. J. Gen. Virol. **78**(Pt. 2):329–336.
13. **Tong, X., and B. A. Malcolm.** 2006. Trans-complementation of HCV replication by non-structural protein 5A. Virus Res. **115**:122–130.
14. **Wakita, T., T. Pietschmann, T. Kato, T. Date, M. Miyamoto, Z. Zhao, K. Murthy, A. Habermann, H. G. Krausslich, M. Mizokami, R. Bartenschlager, and T. J. Liang.** 2005. Production of infectious hepatitis C virus in tissue culture from a cloned viral genome. Nat. Med. **11**:791–796.
15. **Yagi, S., K. Mori, E. Tanaka, A. Matsumoto, F. Sunaga, K. Kiyosawa, and K. Yamaguchi.** 2005. Identification of novel HCV subgenome replicating persistently in chronic active hepatitis C patients. J. Med. Virol. **77**:399–413.
16. **Yoon, S. W., S. Y. Lee, S. Y. Won, S. H. Park, S. Y. Park, and Y. S. Jeong.** 2006. Characterization of homologous defective interfering RNA during persistent infection of Vero cells with Japanese encephalitis virus. Mol. Cells **21**:112–120.

Review

Hepatitis C virus utilizes lipid droplet for production of infectious virus

By Kazuya OGAWA,[*1] Takayuki HISHIKI,[*1] Yuko SHIMIZU,[*1] Kenji FUNAMI,[*1] Kazuo SUGIYAMA,[*2] Yusuke MIYANARI[*3] and Kunitada SHIMOTOHNO[*1,*4,†]

(Communicated by Takao SEKIYA, M.J.A.)

Abstract: Hepatitis C virus (HCV) establishes a persistent infection and causes chronic hepatitis. Chronic hepatitis patients often develop hepatic cirrhosis and progress to liver cancer. The development of this pathological condition is linked to the persistent infection of the virus. In other words, viral replication/multiplication may contribute to disease pathology. Accumulating clinical studies suggest that HCV infection alters lipid metabolism, and thus causes fatty liver. It has been reported that this abnormal metabolism exacerbates hepatic diseases. Recently, we revealed that lipid droplets play a key role in HCV replication. Understanding the molecular mechanism of HCV replication will help elucidate the pathogenic mechanism and develop preventive measures that inhibit disease manifestation by blocking persistent infection. In this review, we outline recent findings on the function of lipid droplets in the HCV replication cycle and describe the relationship between the development of liver diseases and virus replication.

Keywords: hepatitis C virus, lipid droplet, replication, liver disease, VLDL, apolipoprotein

Introduction

Patients infected with hepatitis C virus (HCV) develop acute hepatitis. While 20% of acute hepatitis patients eliminate the virus and recover from the infection, the remaining infectants maintain subclinical state or develop chronic hepatitis as a result of persistent infection. About one-fourth of chronic hepatitis patients progress to hepatic cirrhosis, and half of hepatic cirrhosis patients develop hepatocellular carcinoma (HCC). Many patients with hepatic cirrhosis caused by HCV infection die from the exacerbation of the disease and from HCC. An estimated 15–20% of HCV-infected patients succumb to these hepatic diseases.

Interferon and ribavirin combination therapy is an effective treatment for chronic hepatitis C. Approximately half of patients who complete this therapy eliminate the virus and, therefore, will not develop hepatic disorders thereafter. Generally, it is thought to be difficult to eliminate persistently or latently infected viruses from host. However, in case of HCV, interferon and ribavirin combination therapy can eliminate HCV in half of infected patients, suggesting that HCV infection is more curable with anti-HCV drugs as compared to other persistently infecting viruses. Because persistent virus replication is one of the causes of chronic diseases, a better understanding of the mechanisms of HCV replication, and modification of host cell proliferation by viral infection, will help elucidate the molecular pathogenic mechanism of the disease.

HCV genome and viral proteins

HCV is classified in the *Hepacivirus* genus of the *Flaviviridae* family. Viruses of the *Flaviviridae* family have the positive-sense, single-strand RNA genome that is packaged into an enveloped viral particle.[1)] All the viral proteins are encoded in the largest reading frame in the genome. Translation from the open reading frame of the HCV genome starts by the

*1 Research Institute, Chiba Institute of Technology, Chiba, Japan.
*2 Center for Integrated Medical Research, Keio University, Tokyo, Japan.
*3 Division of Human Genetics, National Institute of Genetics, Shizuoka, Japan.
*4 Professor Emeritus, Kyoto University, Kyoto, Japan.
† Correspondence should be addressed: K. Shimotohno, Research Institute, Chiba Institute of Technology, 2-17-1 Tsudanuma, Narashino, Chiba, 275-0016, Japan (e-mail: kunitada.shimotohno@it-chiba.ac.jp).

doi: 10.2183/pjab.85.217

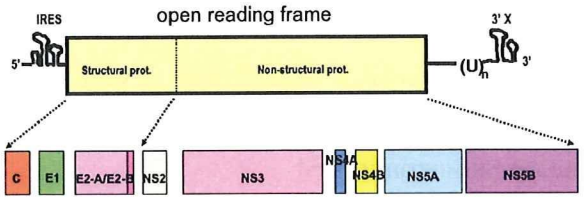

Fig. 1. Structure of the HCV genome and the proteins produced by the genome. The HCV genome (upper panel) consists of a positive-sense RNA strand comprising about 10,000 nucleotides. Virus proteins are first produced as a precursor protein encoded in the largest open reading frame that comprises about 90% of the entire genome, then processed by cellular signal protease(s) followed by two virus proteases which are encoded by NS2-NS3, and NS3, respectively. 5′ one-thirds of the open reading frame encodes proteins for virus particle and the rest encodes non-structural virus proteins that function in virus-infected cells (lower panel).

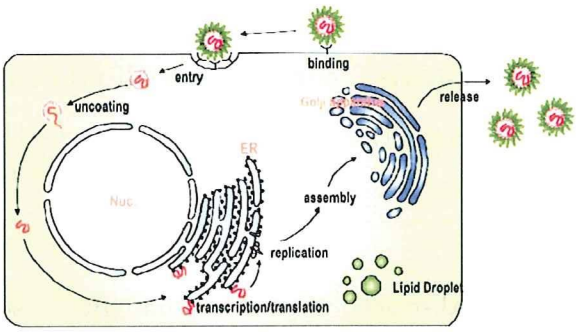

Fig. 2. HCV replication cycle. Since the detailed molecular mechanism of HCV infection/multiplication is yet to be clarified, this figure is drawn as a general view of replication of viruses in *Flaviviridae*, in which HCV is classified. In cells being established virus entry, most of the events for virus replication are conducted in cytoplasm.

mechanism using internal ribosome entry site (IRES) to produce a precursor poly-protein for viral proteins.[2] The precursor poly-protein is subsequently cleaved by a cellular signal peptidase and viral peptidases to produce about 10 different viral proteins.[3),4] Some proteins receive further modification such as glycosylation or phosphorylation to become functionally matured forms. From the N-terminus of the reading frame, Core, envelope1 (E1), envelope2 (E2), p7, non-structural 2 (NS2), NS3, NS4A, NS4B, NS5A and NS5B are produced in this order (Fig. 1). Viral proteins are divided into two categories: structural proteins and non-structural (NS) proteins. The structural proteins compose the virus particle, while the NS proteins function only inside the infected cell and are not packaged in the virion. The HCV structural proteins include the Core, envelope-1 (E1), and -2 (E2) proteins. The remaining NS proteins have unique functions. One important function of the NS proteins is to construct a stage for viral-genome replication and mRNA synthesis by forming a viral replication complex. This replication complex is a specialized structure protected by a cellular membrane that is induced and built by the virus infection. In addition, another type of NS protein complex is thought to contribute to virus particle assembly.

HCV replicates in the cytoplasm of infected cells (Fig. 2). Current models propose that the virus infects a cell by binding to a cell surface receptor, after which the virus particle is endocytosed into the cytoplasm by clathrin-mediated endocytosis. To date, several candidate proteins including virus receptor(s) have been identified as host factors involved in this process. It seems that the LDL receptor and the scavenger receptor class B type I function in the initial stage of HCV infection, after which the HCV particles interact with the tetraspanin CD81 and the tight-junction protein cluadin-1 to establish clathrin dependent internalization.[5)–12)] However, the function of these proteins—from the moment the virus and target cell make contact until infection is established—is not fully understood.

The viral genome replicates in a peculiar membranous structure that is sensitive to detergent around the endoplasmic reticulum[13)–16)]

For most RNA viruses, the viral genome replicates in the environment associating with membrane components of the host cell. It is expected that HCV genome replication also undergoes a process similar to other RNA viruses. While developing the *in vitro* infection and replication system of HCV, the HCV subgenome replicon, which lacks the coding region for structural proteins but carries a drug-resistant marker, is established.[17)] Since this replicon can replicate autonomously, cell lines bearing the subgenome replicon can be selected by selectable marker for *neomycin*. Electron microscopic observation revealed that such cells have an unusual membrane structure and that part of the endoplasmic reticulum (ER) membrane is notably deformed.[13)] This membranous structure has a complicated shape as well as a botryoidal structure in some cases and is also seen in liver specimen from a HCV infected individual.

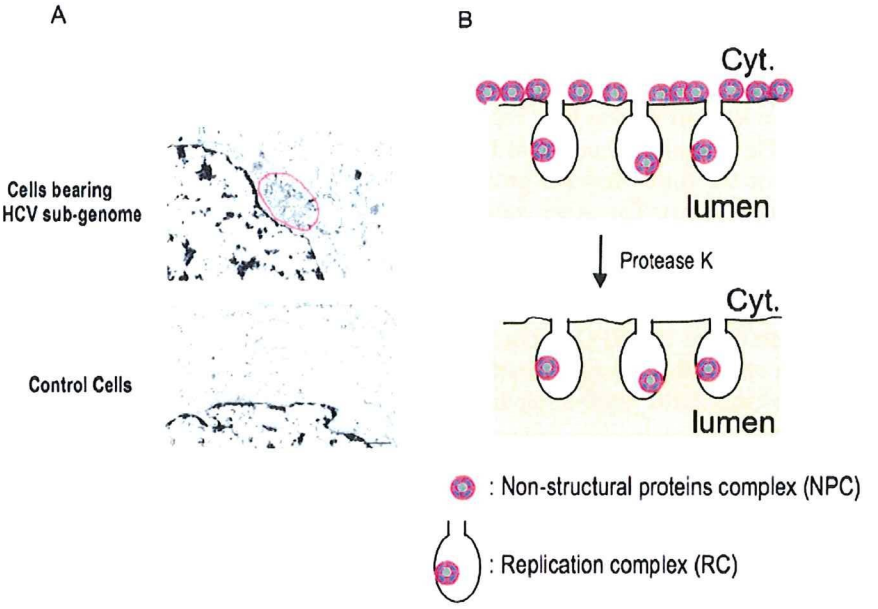

Fig. 3. Altered membranous structure observed in HCV genome replicating cells, in which synthesis of the positive as well as the negative HCV genome is conducted. (A) Electron micrographs of the generation of complex membranous structures (called membranous web) around the ER in HCV genome-replicating cells. The web structure is highlighted by the red circle. (The web image was from Gosert, R *et al.* (2003) J. Virol. **77**, 5487 with permission). (B) Diagram of the distribution of NPC (non-structural proteins complex) and RC (replication complex) around the ER membrane. HCV-genome replicating cells treated with digitonin, a detergent that permeabilizes the plasma membrane but does not affect other membranes (e.g., ER-lumen and nuclear membrane) were analyzed for virus proteins as well as HCV RNA synthesizing activity after incubation of exogenously added protease K. The majority of NS proteins were found to be sensitive to the hydrolysis; only a small portion of NS proteins were found to be resistant to the digestion because of the membrane's protection. Further, the NS protein complex protected by membranous fraction is fully active to synthesize HCV RNA. From this result the NS protein complex exposed to outside of cytoplasm (NPC) and the NS protein complex surrounded with membrane structure (RC) are distinguished and found to have different functions (see text for details).

This structure is called "a membranous web" and is unique to HCV genome bearing cells. Under the labeling condition of *de novo* synthesized RNA, viral-RNA synthesis could be shown to occur around this membranous web.[15] Biochemical analysis of HCV genome-bearing cells was carried out by treating with digitonin, which partially destroys plasma membrane of cells and thus makes cells accessible by exogenous nucleases or proteases present in certain buffer. Through this work the following results were obtained:[14] (1) Surfactants including NP-40 destroyed the replication function of the membranous web; (2) Micrococcal nuclease treatment, under a condition that digests ribosomal RNA completely, did not destroy HCV RNA. However, HCV RNA was immediately destroyed when nuclease treatment was performed in the presence of NP-40, suggesting that viral RNA is protected by membrane components; (3) When digitonin-treated cells were treated with protease K, most viral proteins were hydrolyzed, but about one-tenth or less of the viral proteins remained without being degraded. However, when the protease digestion was performed in the presence of NP-40, the HCV proteins were no longer resistant to protease digestion. This observation indicates that a small portion of the viral proteins is also protected by membrane structures; (4) When digitonin-treated cells were digested with a protease without surfactants, viral RNA synthesis was not affected even when most viral proteins had disappeared. These results suggest that HCV RNA (both positive and negative strands) is synthesized in a membrane-protected complex where only a small portion of the total HCV proteins in cells is present (Fig. 3).[14] Furthermore, the analyses indicate the presence of a protease-sensitive viral protein complex that is not protected by the membranous component in the outer side of the replication complex. It is presumed that

the protease-sensitive complex is directly exposed to the cytoplasm without the protection of the membranous component. Hereinafter, the complex involving viral-genome replication is referred to as the "replication complex" (RC). The complexes consist of HCV RNA and about 10% of the total viral NS proteins in the host cell (data not shown). The other complex that is retained on the membrane structure but directly exposed to the cytoplasmic environment is referred to as the "non-structural protein complex" (NPC). The function of the NPC is not fully understood. Although detailed analyses are still in progress, it is presumed that NPC plays a role in the assembly process of virus particles (see below). A previous study has reported that one of these viral proteins, NS4B, is capable of changing the membrane structure by acting on the ER membrane.[13]

Cytoplasmic lipid droplets play a key role in the production of infectious HCV particles[18]

As mentioned earlier, most HCV proteins localize around the ER membrane in cells that autonomously replicate the HCV genome. In addition, it has been shown that the Core, a structural HCV protein, associates with lipid droplets when it is singularly expressed.[19] It has also been shown that a small portion of NS5A localizes to lipid droplets when NS5A is singularly expressed.[20] What is the relationship between the intracellular location of viral proteins, particularly the association of Core and NS5A with the lipid droplet, and viral replication? To understand this phenomenon, we also analyzed the role of Core association with the lipid droplet in virus reproduction using a cell-culture system that produces an infectious virus.[18]

When infectious clone JFH1 of HCV genomic RNA is introduced into HuH7 cells (a human liver cancer-derived cell line), genome replication begins and virus particles are produced.[21] Analysis of the buoyant density of virus particles determined by a sucrose density-gradient centrifugation method indicates the presence of two types of HCV. Most viral particles were detected in a fraction of 1.15 g/ml density, but these particles were not infectious to HuH7 cells. On the other hand, a small amount of infectious virus particles was detected in a 1.12 g/ml density fraction (Fig. 4). In the HCV-replicating cells, the core protein was found to localize around lipid droplets similar to a previous report that identified it via an experiment on the solitary expression of Core proteins in cells.[19] In addition, many of the NS proteins (NS3–NS5B) were co-localized to the ER as previously reported. However, detailed examination revealed that the NS proteins localized around the lipid droplets as well as ER.[18] HCV RNA could also be detected around the lipid droplets. The fraction containing lipid droplets, partially purified by floating centrifugation method, was capable of supporting HCV RNA synthesis. Furthermore, the surrounding environment of the lipid droplets in HCV replicating cells is rich in membrane-like structure (see below). This accumulation of membranous structures around the lipid droplet is unique to the infected cells and is not observed in uninfected control cells.

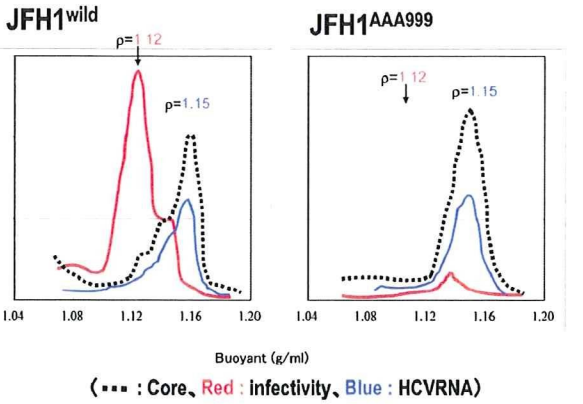

Fig. 4. Characteristics and infectivity of virus particles produced into the culture supernatant. The characteristics of virus particles released from HCV(JFH1^{wild})-replicating cells (left) or cells replicating a mutated virus, JFH1^{AAA999}, encoding proteins that cannot associate with lipid droplets (right) were analyzed by the sucrose density gradient centrifugation method. Dotted, red, and blue lines indicate the amount of virus particles measured by the amount of viral core protein, infectivity and viral RNA, respectively. Buoyant density of sucrose is indicated.

Core proteins promote the localization of NS proteins to lipid droplets[18]

In cells bearing the defective HCV genome not expressing the core protein, the NS proteins were mainly localized on the ER and were not seen around the lipid droplet. However, in cells producing the infectious virus, the NS proteins were localized to both lipid droplets and the ER membrane. The Core and other structural proteins (E2), co-localized to lipid droplets. It is worth noting that the Core promotes the localization of the NS proteins to lipid droplets. This was found using the defective HCV genome

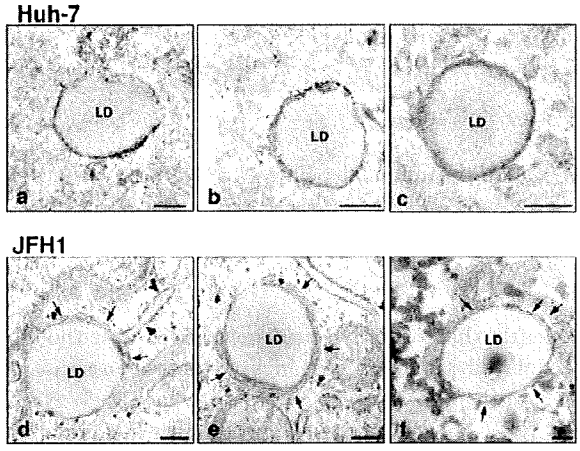

Fig. 5. Membranous structures are frequently observed around the lipid droplets in JFH1-bearing cells. Electron micrographs of the lipid droplets and the surrounding area are shown. These show different images of lipid droplets in cells; a to c, lipid droplets in control HuH-7 cells, and d to f, those in JFH1 bearing HuH7 cells. Arrows indicate enriched membrane structure around the lipid droplet. Arrowhead shows rough ER membrane-like structure attached to the lipid droplet (The data was from Miyanari *et al.* (2007) Nat. Cell Biol. **9**, 1089 1097).

that does not express the Core. When this mutant genome was expressed, NS5A localized to the ER but not to the lipid droplet. However, when the Core was provided exogenously into the cells, both NS5A and the Core were co-localized to the lipid droplets. Association of other HCV NS proteins with the lipid droplets was also observed by Core dependent manner. This suggests that the Core recruits NS proteins to the lipid droplets, although the mechanism for this association in the presence of Core is unclear.

HCV proteins are arranged in order around lipid droplets in laminae according to protein type

When HCV Core-dependent association of viral NS proteins to the lipid droplets was examined by confocal light and electron microscopy, the Core was shown to be directly localized on the surface of the lipid droplets. However, NS5A was mainly observed in the membranous structure that surrounds the Core-coated lipid droplets.[18] This membrane structure is not of the lipid droplet. More specifically, the Core could be seen as a lamina surrounding the lipid droplet, and the membranous components that are rich in NS proteins surrounded the Core-coated lipid droplets. While examining intracellular localization and behavior of the Core-coated lipid droplets, majority of Core coated-lipid droplets were found to reside near the ER around the nuclear membrane (data not shown).

Abnormal membrane structures are enriched around lipid droplets in HCV-producing cells

Regarding generation of lipid droplet, several mechanisms have been proposed.[22),23)] One mechanism is that ER accumulates neutral fat, mainly triglycerides and cholesterol ester, in the space of the membrane bilayer. Increasing the lipid contents increases the mass of the body and the lipid droplet covered with ER-derived membrane buds from the ER.[22)] The membrane structure of the lipid droplet is, thus, monolayer. Lipid droplet-specific proteins (such as TAP: TIP47, ADRP and Perilipin) associate with the monolayer membrane of the lipid droplet. This typical structure of the lipid droplet can be seen in human liver cancer-derived cell line, HuH7 (Fig. 5). However, in HuH7 cells where the infectious HCV genome could replicate and produce virus particles, a part of surface of the lipid droplets were often seen to be covered with several layers of membrane (Fig. 5). Moreover, complicated membrane structures accumulated around the lipid droplets. Although the origin of these membrane structures is unknown, it is assumed that they are derived from ER membranes because the Core-coated lipid droplets are frequently observed around the ER. The ER membranes are also rich in NPC and RC of HCV as shown in the graphic of Fig. 6(A).

Functional analysis of lipid droplets in virus production using the mutated viral genomes

How does the association of viral proteins around the lipid droplets affect virus production? Previously, the domain of the Core to interact with the lipid droplet is disclosed.[24),25)] Mutations of two proline residues to alanine in that region of Core, $Core^{PP/AA}$, no longer associate with the lipid droplet.[25)] When the mutated viral genome that produces $Core^{PP/AA}$ is introduced into cells, the Core as well as HCV NS proteins no longer localize around the lipid droplets.[18)] This result indicates that the Core, which is able to associate with the lipid droplet, functions to recruit other viral proteins to the lipid droplets. The cells expressing this mutant genome do not produce virus particles in the culture medium. Under

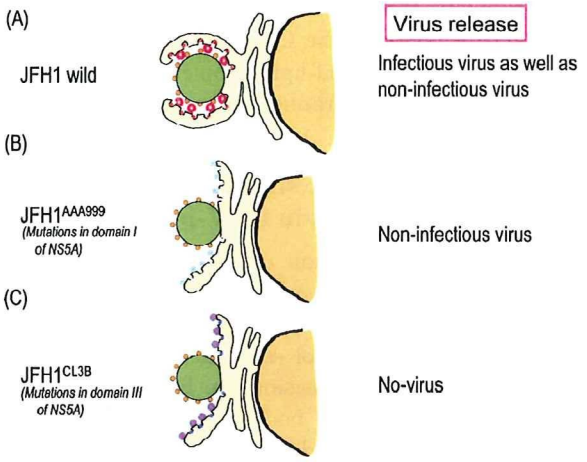

Fig. 6. Model of the association of the Core-coated lipid droplets with NPC- and RC-rich endoplasmic reticulum. Association of Core-coated lipid droplets with RC- and NPC-rich ER in HuH7 cells bearing the infectious HCV genome, JFH1 (A). Association of Core coated-lipid droplets with the lipid droplet was not observed in cells bearing the mutant JFH1, JFH1^{AAA999}, expressing NS5A with mutations in domain-I (B),[18] and in cells bearing the mutant JFH1, JFH1^{CL3B} encoding NS5A with mutations in domain-III (C).[28] Green circles represent lipid droplets. The small orange circles around the lipid droplets are the Core. The largest and the smallest circles with a mosaic represent NPC and RC, respectively. The color of NPC and RC indicates the noted mutations in NS5A in these complexes. Note that the NPC- and RC-rich ER lobes with a mutant NS5A (B and C) do not associate with the core-coated lipid droplet. However, as shown in (B) noninfectious virus particles are released into the culture medium, while NPC and RC with mutations in domain-III of NS5A do not produce virus particles, indicating the lack of virus assembly with this mutant. For NPC and RC localization, see the graphic in Fig. 3.

these conditions, virus production may be inhibited due to lack of association of viral proteins with the lipid droplet that is probably a prerequisite for virus production or virus assembly, or, the mutated Core itself is no more able to execute morphogenesis of virus particle.

An experiment was performed to examine whether or not the association of Core and HCV non-structural proteins to the lipid droplet is essential to virus particle formation.[18] For this purpose the HCV genome with mutation in an NS protein was constructed. NS5A was selected for introducing the mutation among other non-structural proteins as NS5A associates with the lipid droplets more frequently than other NS proteins and, thus, is thought to play a proactive role in lipid droplet association with other NS proteins. As shown in Fig. 7, NS5A of HCV-1b genotype is a protein with 466-amino-acid residues that can be divided into three domains (domain-I, -II, and -III from the N-terminus). Mutations were introduced into domain-I using alanine-scanning mutagenesis. NS5A mutants that are not severely interfered with genome replication, but fail to associate with lipid droplet were selected among the mutants. By doing so, NS5A mutant in which amino acid residue, APK, of 99-101th or, PPT, of 102–104th, was converted to 3 consecutive alanine residues. When the viral RNA genomes encoding one of these NS5A mutants were introduced into cells and virus production to culture medium was examined, only noninfectious virus particles with 1.15 g/ml buoyant density were produced (Fig. 4).[18]

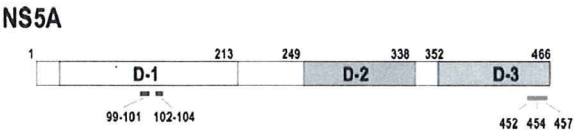

Fig. 7. Structure of the HCV NS5A protein and mutant NS5A used for the analysis described in this paper.[18),28)] D-1- D-3 indicates domain-I - domain-III.

This result confirmed the importance of the lipid droplet for production of "infectious" virus particle. It is likely that infectious virus production requires aggregation of NPC- and RC-rich structures derived from the ER membrane around the lipid droplets. Cells with these structures produced both infectious and noninfectious particles. However, cells bearing the viral genome with mutations in NS5A that failed to associate with the Core-coated lipid droplet produced virus particles that lacked infectivity. Thus, it is likely that lipid droplets play a key role in generating infectious viral particles. Meanwhile, mutants with deletions or point mutations in domain-III in the C-terminus of NS5A had no defect in genome replication but were unable to associate with Core-coated lipid. Neither infectious nor noninfectious viral particles were produced from these cells bearing the genome having these mutations.[26)–28)]

This observation suggests that NS proteins, which constitute NPC around the Core-coated lipid droplet, are involved in the assembly of infectious virus particles.[18),26)–28)]